SCIENTIFIC CULTURE

www.sci-cult.com

DOI: 10.5281/zenodo.20703612

SCIENTIFIC CULTURE, Vol. 12, No.5, (2026), pp. 1007-1037
Open Access. Online & Print

METAHEURISTIC OPTIMISATION OF SHUNT ACTIVE POWER FILTER CONTROL FOR POWER QUALITY ENHANCEMENT IN HYBRID RENEWABLE MICROGRIDS

Gagan Kumar Sahoo[1] and Subhashree Choudhury[2*]

[1] *Department of Electrical Engineering, Siksha 'O' Anusandhan (Deemed to be) University, Bhubaneswar, Odisha-751030, India*

[2] *Department of Electrical and Electronics Engineering, Siksha 'O' Anusandhan (Deemed to be) University, Bhubaneswar, Odisha-751030, India*

[*]***Correspondence:*** *Subhashree Choudhury (email: subhashreechoudhury@soa.ac.in)*

Abstract: The growing global demand for electricity, driven by rapid industrialisation and population growth, has intensified the need for sustainable and high-quality power systems. Hybrid renewable energy source (HRES)–based microgrids provide a practical pathway for integrating clean energy; however, the widespread use of nonlinear loads and power electronic interfaces introduces persistent power quality challenges, including harmonic distortion, voltage sags, and unbalanced fault conditions. In this study, an intelligent optimisation-based control strategy for a shunt active power filter (SAPF) is proposed using the Mountain Gazelle Optimiser (MGO), a recently developed bio-inspired metaheuristic algorithm, to tune proportional–integral (PI) controller gains dynamically. The MGO-optimised PI controller adaptively regulates inverter switching signals to enhance harmonic mitigation, reactive power compensation, and overall system stability. A detailed MATLAB/Simulink model of a grid-connected hybrid photovoltaic–fuel cell–battery microgrid is developed to assess the proposed approach under severe power quality disturbances, including voltage sag events and line-to-line-to-ground faults. Simulation results demonstrate that the MGO-based SAPF achieves substantial performance improvements over conventional PI control, including a 42.53% reduction in total harmonic distortion under fault conditions, an 8.08% improvement during voltage sag events, an 80.87% reduction in voltage deviation, and a 3.45% enhancement in power factor, while maintaining compliance with IEEE 519 standards. These results highlight the effectiveness of the proposed MGO-PI control framework as a robust, adaptive power-conditioning solution for enhancing power quality in renewable-rich microgrids and supporting the operational requirements of future intelligent energy systems.

Keywords- Hybrid Renewable Energy Sources (HRES); Machine Intelligence; Shunt Active Power Filter (SAPF); Mountain Gazelle Optimiser (MGO); Power Quality (PQ) Enhancement; Grid-Tied Microgrid; Metaheuristic Optimization; Intelligent Control

Introduction

1.1 Overview

Recently, electric power networks have faced numerous challenges, particularly the reliance on fossil fuels and thermal power generation, which have led to high costs, pollution, and resource depletion [1]. Researchers have advocated for renewable energy sources (RESs) to address these issues due to their advantages, including environmental sustainability, abundant availability, energy security, lower transmission losses, lower operating expenses, and their role in reducing emissions and mitigating global warming [2]. Additionally, population growth and industrial development have significantly

increased electricity demand. Hybrid renewable energy sources (HRESs) are being integrated into the grid to address this demand, enhance reliability, minimise losses, and reduce fossil fuel use, thereby contributing to environmental degradation [3]. Various HRESs, such as photovoltaic (PV) [4], fuel cells (FC) [5], wind power [6], and biomass [7], are combined with localised energy usage and storage systems to form microgrids (MGs), which are local electric networks [8].

This study emphasises PV-based RES due to its several benefits, including (1) zero fuel expenses, (2) scalable power generation, (3) easy installation on rooftops, (4) minimal upkeep, (5) widespread availability, (6) eco-friendliness, (7) high dependability, and (8) silent operation [4]. To enhance efficiency, FC is integrated with PV for its notable features such as (1) user-friendliness, (2) improved performance, (3) reduced harmful emissions, (4) modular structure, (5) combined heat and power (CHP) potential, (6) greater stability, and (7) cost efficiency [5]. However, PV/FC systems have limitations, including PV's dependence on weather conditions, FC's slow response, and rising material costs at elevated temperatures, which make them less viable. To overcome these drawbacks, this research proposes incorporating battery storage, known for its superior energy retention [9], with PV/FC to effectively meet electricity requirements while enhancing system efficiency, fuel optimisation, resilience, and dependability.

1.2 Motivation

Integrating HRESs into the Microgrid network introduces several challenges to stability and safe operation. These difficulties arise from the fluctuating nature of RESs, the varying AC/DC output types, the diverse voltage levels from different sources, and their dependence on environmental conditions [10]. A solution to these issues lies in using power-electronics interfaces (PEIs), which can optimise energy harvesting from each HRES and convert the DC output to AC for seamless integration with the grid [11]. However, using PEIs in MG systems raises various power quality (PQ) concerns, including harmonic distortion and system disturbances [11]. These disruptions can damage the source and grid machinery, leading to malfunctions and potential overheating. Common PQ problems identified in the literature include harmonics, voltage sags, voltage swells, interruptions, oscillatory transients, flickers, notches, LLG, and frequency deviations [12]. To ensure reliable and secure MG functioning, mitigating and effectively managing these PQ disturbances is crucial. Due to the non-linear characteristics of PEIs, advanced control strategies are necessary to enhance power quality while achieving other control objectives, such as voltage, frequency, and power flow regulation.

1.3 Literature Survey

This section discusses a comprehensive assessment of existing works on numerous control methods for optimally regulating MG networks, focusing on optimising resource utilisation, ensuring rapid transient behaviour, enhancing voltage stability, and boosting overall system performance.

Researchers have proposed a control approach in [13] for PQ improvement in MG by employing a state-feedback controller to manage imbalanced and nonlinear loads and electric springs to enhance the voltage profile. The hybrid strategy improves MG effectiveness and consistency by affirming proper load balance, robust reactive power control, and overall voltage stability. In [14], a control approach for PQ advancement in a Hybrid AC/DC Microgrid has been reported, utilising an interlinking converter. The authors have combined an optimised ANFIS and a GRU-based controller to regulate DC voltage, reduce harmonics, and improve the power factor in an MG system integrated with a PV-UPQC [15]. A PQ augmentation technique has been recommended by Srividhya et al. [16] for smart MGs, incorporating a Convolutional Neural Network (CNN) and an Interline Power Flow Controller (IPFC). The IPFC coordinates power flow between buses, and the CNN estimates and counterbalances for power interruptions. Shravani and Narasimham have proposed a complementary UPQC scheme with a Self-Compensating Sine Oscillator (SCSO) to develop PQ in MGs by mitigating voltage swells, sags, and disruptions. Simulation results confirm its effectiveness for smart microgrid integration [17]. Brahmendra

Kumar et al. have proposed a hybrid energy storage system with ramp-rate control to improve power quality in grid-connected PV microgrids. The system stabilises voltage, reduces harmonics, and enhances power quality, as demonstrated through simulations and Hardware-in-the-Loop testing [18]. Researchers in [19] have introduced a 72-pulse inverter-based Unified Interphase Power Controller (UIPC) to improve power flow and quality in residential-industrial microgrids. The system uses a dual-loop control strategy to stabilise voltage, minimise harmonic distortion, and optimise power flow. Simulation results demonstrate enhanced power quality, reduced THD and improved voltage regulation. Artemenko et al. have discussed power quality assessment and improvement in grid-tied distributed generation systems, proposing an extended instantaneous power theory. They also explore methods like power electronics and control strategies to address voltage sags, harmonics, and reactive power imbalances [20]. In [21], the adaptive Hybrid Voltage and Current Controlled Method is proposed to enhance the efficiency of harmonic compensation using distributed resources. This approach can substantially reduce the need for low-pass filters at the distributed resource side. A multi-objective technique based on fuzzy decision-making has been proposed by B. Cao et al. for a hybrid MG to achieve a proper balance among incompatible targets, such as consistency, price, and ecological effects [22]. Further, this method enriches versatility and completeness in MG configuration and intervention. An integrated methodology employing the Artificial Bee Colony (ABC) algorithm and a modified fuzzy logic controller (FLC) has been proposed in [23] for optimising MPPT in solar systems to achieve advanced tracking and efficiency under varying conditions.

Electrical conditioning equipment, such as uninterruptible power supplies, active power filters, and static var compensators, plays a crucial role in mitigating PQ anomalies in MGs, rectifying voltage oscillations, and eradicating distortions, thereby guaranteeing a consistent and resilient power supply. They efficiently address PQ issues typically caused by the addition of intermittent sources, such as PV and wind, and by changing loads, thereby enhancing PQ performance and stability in MG systems [24-25]. In [26], the authors present an efficiency excellence control framework for MGs by coordinating a UPQC with Distributed Energy Resources (DERs). Simulation findings demonstrate the efficacy of the hybrid method in robustly mitigating PQ issues, power mismatch, voltage regulation, and current compensation. The competence of Static VAR Compensators (SVCs) combined with intelligent automation techniques has been projected in [27] for improving transient response stability in MGs. Power quality improvement in a grid-tied hybrid energy system using D-STATCOM controlled by the Grasshopper Optimisation Algorithm (GOA) has been discussed in [28]. The D-STATCOM mitigates issues such as voltage fluctuations and harmonics, while the GOA optimises control parameters for improved performance. Simulation results show enhanced voltage stability, reduced THD, and improved overall power quality. Researchers have deployed a coordinated control of flywheel [29] and battery storage as power conditioning devices to improve frequency regulation in diesel-based microgrids. The flywheel handles rapid changes, while the battery maintains long-term balance, resulting in improved stability, reduced generator stress, and enhanced overall performance [30]. Authors in [31] have implemented an innovative, multi-purpose superconducting equipment for DC MGs, integrating SMES and SFCL that enhance voltage stability and system predictability by efficiently storing and discharging energy during fault current suppression.

Shunt Active Power Filter (SAPF) is regarded as a potent Electrical conditioning equipment for effectively mitigating PQ issues in MGs [32]. It works effectively by compensating for PQ disturbances, reactive power, and load imbalance, thereby enhancing voltage regulation, improving power factor, reducing losses, and safeguarding sensitive devices susceptible to power anomalies. Furthermore, SAPFs provide a resilient approach for contemporary power grids, offering rapid adaptive performance, configurability, and the ability to respond to changing load conditions. A comprehensive analysis and study of various control methods for SAFP to enhance PQ have been meticulously projected in [33]. The article also analyses realistic deployments of SAPFs in industrial-scale, corporate, and renewable power systems, and projects their flexibility and performance under different load conditions. Authors in [34] have designed a novel control approach for a SAPF that combines it with a high-selectivity filter to improve harmonic detection and reactive power compensation. A robust control strategy has been designed for SAPFs to enhance PQ in islanded and grid-tied MGs [35]. Srivastava and Saravanan [36] proposed an optimal supervisory method for SAPF-based EV charging stations to achieve harmonic reduction and PQ improvement. In [37], ADRC-based control for an autonomous PV, Wind, and Battery MG hybridised with a SAPF has been proposed under varying load conditions to improve stability and reduce oscillations. In [38], a novel Sliding Mode Controller (SMC) has been implemented with a SAPF in an islanded MG to improve PQ indices and voltage steadiness, thereby ensuring the reliability of grid operation under load uncertainty. A synergetic control method for a 3-level voltage-source inverter-based SAPF has been proposed in [39] to improve PQ, ensure proper harmonic settling, achieve robust reactive power control, maintain adequate voltage regulation, and provide a quicker response than conventional techniques. In [40], the authors implemented a coordinated Resistive Superconducting Fault Current Limiter (RSFCL) and a fuzzy-based SAPF to improve PQ in MGs. This approach enhances fault current limiting, harmonic compensation, and voltage regulation, thereby improving the dynamic stability and power quality of microgrid operations.

Some studies have highlighted the widespread adoption of conventional controllers, such as Proportional Integral (PI) and Proportional Integral Derivative (PID), due to their simple design, low cost, and rapid computational efficiency. Nevertheless, their linear nature limits their ability to handle PQ disturbances effectively. To enhance their performance and to determine the optimal control parameters for these linear controllers, various optimisation techniques such as Modified Water Wave Optimization [41], Improved Bat Algorithm and Moth Flame Optimization Algorithm [42], Puzzle Optimization Algorithm [43], Hybrid Jellyfish Search Optimizer and Particle Swarm Optimizer [44], Mexican Axoltl Dingo Optimize [45], Green Leaf-Hopper Flame Optimization [46], Amended Penguin Optimization Algorithm [47], Chaotic Butterfly Optimization [48], etc have been reported in the literature [32]. Authors in [49] have proposed a PV-fed UPQC with an adaptive PI controller using a modified JAYA algorithm for real-time tuning. Unlike conventional fixed-gain PI methods, the dual-objective JAYA approach improves current and voltage quality under dynamic conditions, outperforming traditional techniques. The authors have discussed a comparative strategy employing PI and fuzzy controllers for PQ optimisation. They evaluate both voltage regulation and harmonic reduction methods and conclude that the fuzzy controller offers superior adaptability and control accuracy compared to the traditional PI controller [50].

Real-world problems are often complex and require approximate optimisation methods. While heuristic techniques have a limited scope, meta-heuristic algorithms are more versatile and can handle diverse, non-linear problems. Though they don’t guarantee the best solution, they deliver acceptable results more quickly by balancing exploration (broad search) and exploitation (focused search). However, issues such as low convergence and difficulty with local optima persist. The "No Free Lunch" theorem highlights that no single algorithm can solve all problems optimally, leading to the rise of nature-inspired metaheuristics [51-54]. Driven by the ongoing quest for more effective optimisation strategies, Benyamin Abdollahzadeh introduced the Mountain Gazelle Optimiser (MGO) in 2022, inspired by the social behaviour and survival strategies of wild mountain gazelles [55]. MGO models four key behavioural phases: mother-offspring interaction, single male dynamics, territorial solitude, and foraging movements, each contributing to the algorithm's search capabilities. This nature-inspired meta-heuristic demonstrates robustness and adaptability, offering several notable advantages like [56-58]: (1) effective balance between exploration and exploitation; (2) accelerated convergence rate; (3) high adaptability to complex, high-dimensional problems; (4) strong diversity preservation; (5) independence from derivative information; (6) simplicity and ease of implementation; (7) broad applicability across various domains; and (8) stochastic escape mechanisms that improve the ability to avoid local optima.

After a thorough review of the merits of Shunt Active Power Filter (SAPF) and the nature-inspired meta-heuristic optimisation (MGO) method, the authors identify a gap in the literature regarding the dynamic tuning of PI control parameters for SAPF using the MGO technique. This has not been extensively explored in previous research. To address this, the authors propose an innovative approach that combines the MGO technique with SAPF to enhance harmonic mitigation, reactive power compensation, and voltage regulation. The MGO method, with its ability to strike an optimal balance between exploration and exploitation, ensures accelerated convergence and high adaptability to complex, high-dimensional problems. By dynamically tuning the PI parameters, the approach enables precise control of the gate pulses in the inverter circuit. This results in a more efficient, robust, and flexible control strategy that improves power quality, system stability, and adaptability to varying load conditions in modern power networks.

1.4 Significant Achievements

Although several studies have addressed PI controller design and SAPF operation to improve power quality, a research gap remains in optimally tuning PI parameters using advanced metaheuristic algorithms under severe grid-fault conditions, such as SAG and LLG faults, in hybrid renewable microgrid environments. Existing works often lack a comprehensive analysis of grid voltage and current harmonics, failing to provide detailed numerical and graphical evidence in such challenging scenarios. This study aims to bridge this gap through the following significant achievements:

1) The existing studies primarily address power quality (PQ) enhancement either at the load end (Point of Common Coupling - PCC) or at the source terminals. However, none have comprehensively focused on simultaneously improving PQ using a unified control strategy at both locations. This research bridges that gap by ensuring effective PQ enhancement at both source and load terminals through a standardised control approach.

2) This study employs a Shunt Active Power Filter (SAPF) to mitigate short-term voltage disturbances. The PI controller parameters are optimally tuned using the proposed robust Mountain Gazelle Optimiser (MGO) algorithm. The MGO-based tuning ensures superior PQ, improved system performance, and enhanced reliability. The algorithm exhibits several key advantages, including:

✓ Balanced exploration and exploitation capabilities
✓ Rapid convergence
✓ Adaptability to high-dimensional optimisation problems
✓ Effective diversity preservation
✓ Independence from derivative information
✓ Simplicity in implementation
✓ Broad applicability across various systems
✓ Erratic escape mechanisms that enable it to avoid local optima effectively.

3) To validate the performance of the proposed MGO-controlled SAPF, rigorous fault scenarios are introduced, specifically i) voltage sag and ii) three-phase line-to-ground (LLG) faults at the PCC, occurring between 0.4 and 0.6 seconds. The controller's effectiveness under these fault conditions is analysed and compared with that of the conventional PI controller, demonstrating notable improvements.

4) The proposed MGO technique also manages fluctuations on the input source side by regulating the solar array's output, the FC, and the State of Charge (SoC) of the battery. This ensures a more robust and stable performance than traditional PI-controlled SAFP MG systems.

5) A detailed evaluation of the simulation outputs highlights the elevated capability of the MGO-based PI controller in maintaining key parameters such as DC link voltage, terminal voltage, voltage deviation, power factor, and frequency stability amid extreme disturbances like voltage sags and LLG faults. Additionally, the proposed strategy ensures that the active, reactive, and apparent powers remain nearly constant, with minimal oscillations, under fault conditions. This results in superior power delivery characteristics for the microgrid (MG). The method also significantly reduces total harmonic distortion (THD), aligning with IEEE standards, and outperforms conventional PI control methods in mitigating voltage instability and harmonics.

6) Deploying the proposed controller and SAPF-PI ensures effective regulation of grid voltage and current, significant reduction in harmonic distortion, and improved transient stability. These enhancements collectively improve the system's overall efficiency and reliability, thereby validating its potential for real-time implementation.

1.5 Paper Structure

The following is a summary of the entire research paper. Section 2 details the mathematical framework for the HRES, which comprises PV, FC, battery, and SAPF-based MG systems. The suggested and classical control methods are elaborately analysed in Section 3, featuring mathematical ideas and flowcharts. The discussion of the MATLAB/Simulink model and comprehensive results is presented in Section 4. The detailed research findings are discussed in Section 5, and Section 6 presents the concluding remarks of the entire research work. Future directions are discussed in detail in Section 7, emphasising cutting-edge technologies, creative ideas, and interdisciplinary teams to address new problems and enhance existing ones. In Fig. 1, a schematic representation of the entire investigation is depicted, showcasing the key concepts.

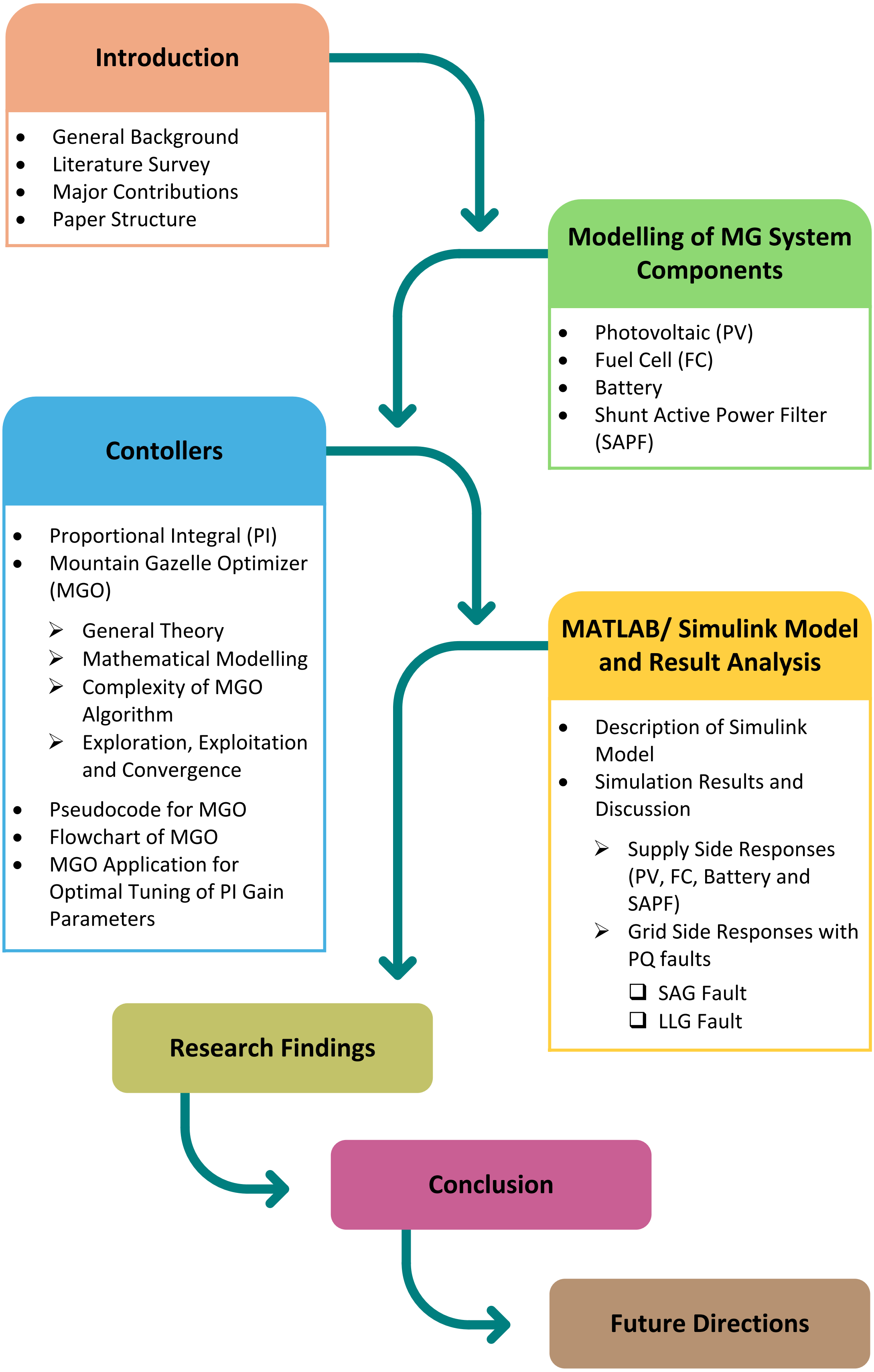

Fig.1. Schematic representation of the entire investigation showcasing the key concepts

2. Modelling of System Components

In order to illustrate the effectiveness, dependability, and robust performance of the suggested MGO method, a PV, FC, battery-based HRES for an MG network has been considered for this study and established in the Simulink environment. All system components, including the PV, fuel cell, battery, and SAPF, have also been thoroughly modelled and explained.

2.1 Photovoltaic (PV)

PV systems work by using solar irradiance as their energy source to convert solar energy into electrical power. Due to its eco-friendliness, lack of noise pollution, low maintenance needs, and lack of fuel consumption, photovoltaic systems (PVs) are recognised as one of the most essential renewable energy-based distributed energy resources [1,2]. Photoelectric current is produced when electrons are excited by solar radiation and fall on a solar cell's surface. PV cells are joined in series and parallel configurations to produce PV modules. A PV array that acts like a current source comprises several PV modules connected systematically. This study examines a PV cell's single-diode model. The PV panel generates photoelectric current, which is technically denoted as [3]:

$$I_{Cell} = I_{Ph-Cell} - I_0\left[exp\left(q^{\frac{V_{Cell}+I_{Cell}R_S}{\beta\sigma T_{OP}}} - 1\right)\right] - \frac{V_{Cell}+I_{Cell}R_S}{R_{Sh}} \quad (1)$$

2.2 Fuel Cell (FC)

A fuel cell is an electrolytic device which uses electrochemical operations at the cathode and anode to transform chemical energy from an oxidising agent and fuel source into electrical energy [4]. Fuel cells (FCs) are necessary distributed energy resources because they can produce power continuously for long periods, provided that fuel and oxygen are available. Researchers in the literature have identified numerous FC types. Because of its many benefits, among all the Proton Exchange Membrane Fuel Cell (PEMFC) is regarded as the most cost-effective of them all due to the following advantages: (1) simplicity of use; (2) increased effectiveness; (3) decreased harmful toxins; (4) augmented modular design; (5) considerable potential for combined heat and power (CHP); (6) improved stability; (7) affordability; (8) fuel flexibility; 9) prompt startup; 10) lightweight design; 11) compact structure; and (12) solid electrolyte [4]. A FC 's fundamental component is an electrolytic substance positioned between the cathode (negative electrode) and the anode (positive electrode). The electrochemical reactions taking place at the anode and cathode can be mathematically represented as in equations (2) and (3) respectively [5]:

$$H_2 = 2H + 2e^- \quad (2)$$

$$2H + \frac{1}{2}o_2 + 2e^- = H_2O \quad (3)$$

The entire electrochemical reaction occurring in the FC is given by:

$$\frac{1}{2}O_2 + H_2 = H_2O + Heat\ Energy + Electricity \quad (4)$$

2.3 Battery

Batteries are well-known and high-capacity energy storage devices with extensive applications in several electrical fields, as they possess many advantages. 1) They give the system a significant boost and a steady voltage, and 2) by absorbing or adding electricity to the load during frequency changes, they can also control frequency [6]. Batteries are made up of elements that transform chemical energy into electrical energy and vice versa. Under typical operating circumstances, the battery unit can store electrical energy, which can be utilised to deliver energy during shortages or outages [7]. There are different varieties of battery storage systems, like 1) lithium-ion (Li-ion), 2) lead–acid, 3) nickel–metal hydride (Ni-MH), 4) nickel-cadmium (Ni-Cd), etc. In this research work, Li-ion is employed due to many merits such as: 1) improved self-discharging capability, 2) enhanced efficiency, 3) increased number of charging and discharging cycles, 4) more energy density, 5) economical, etc [6]. Applying Kirchhoff's Voltage Law (KVL) to a simple Li-ion battery configuration consisting of a voltage source, capacitors, and resistances can be mathematically represented as [8]:

$$V_T(t) = V_{OC}(z(t)) - V_1(t) - V_2(t) - R_S I(t) \quad (5)$$

2.4 Shunt Active Power Filter (SAPF)

Compensating currents are introduced into the distribution network to counteract reactive power, harmonics, and other distortions caused by nonlinear loads. SAPFs actively monitor the power system by creating currents that neutralise unwanted elements, boosting voltage stability, decreasing losses, and improving overall system efficiency, resulting in improved MG system PQ. Typically, SAPFs are linked in parallel (shunt) to the load [9]. SAPF brings about harmonic cancellation, reactive power compensation, power factor improvement, proper voltage regulation, load balancing, mitigation of oscillations, and an overall increase in the MG system efficiency when PQ faults occur. The general compensation principle of SAPF has been illustrated in Fig.2. The detailed operation and control structure of a SAPF has been demonstrated in Fig.3 [10].

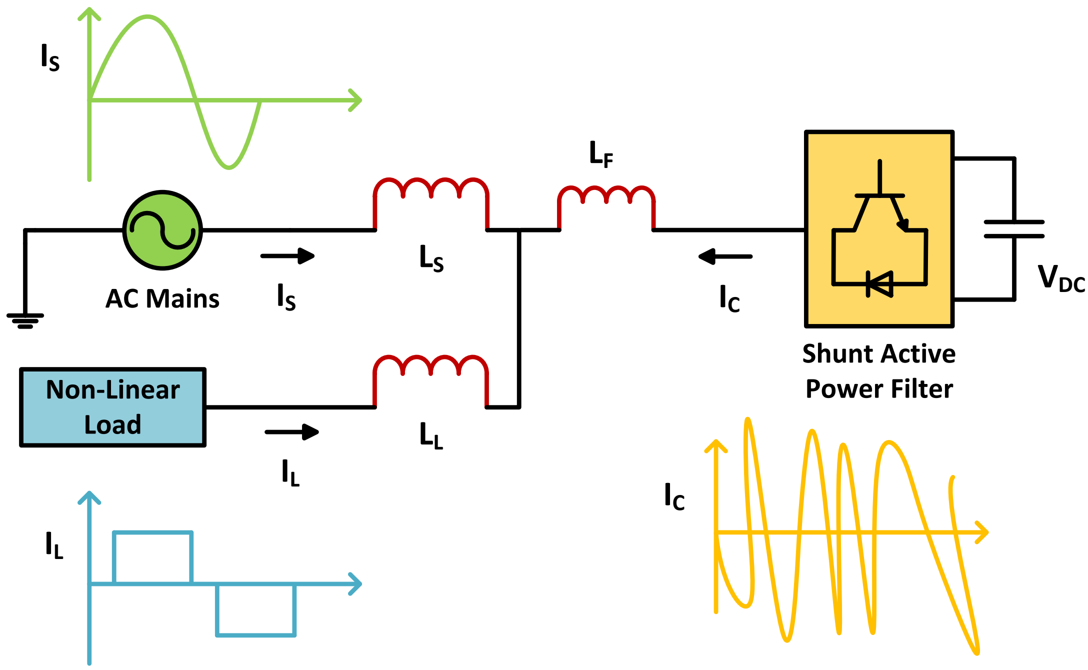

Fig.2. Mechanism of SAPF Power Compensation

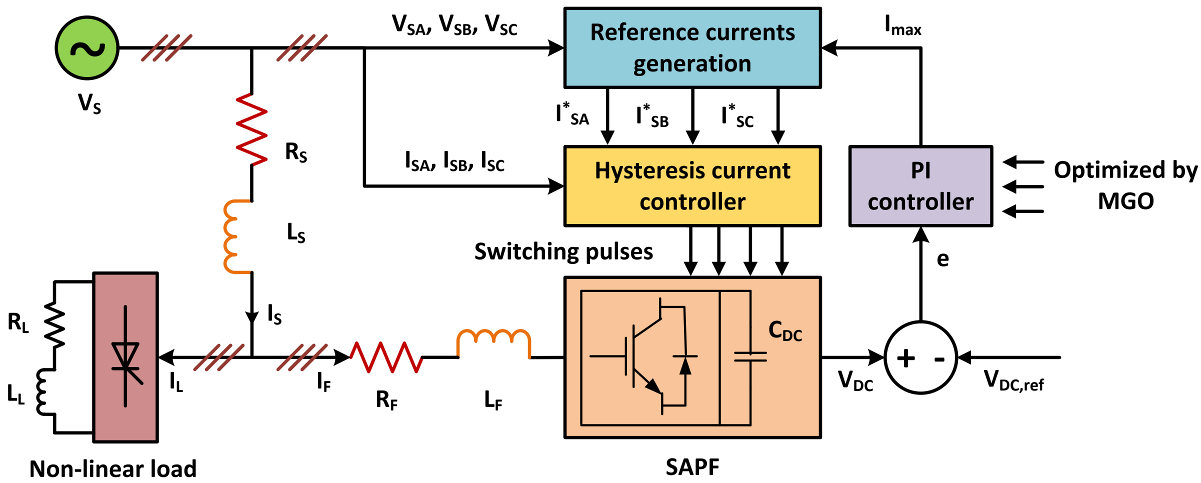

Fig.3. SAPF Operational Framework and Control Design

3. Controllers

3.1 Conventional Proportional Integral (PI) Controller

A Proportional Integral (PI) controller exists as a traditional, unidirectional, feedback-loop control technique that is simplest to employ. It comprises gain values K_p and K_i, for the proportional (P) and the integral (I) controller, respectively. K_i reduces the steady-state error while K_p increases the rising time, resulting in an efficient total control action [11]. A PI controller is employed in the SAPF circuit to drive the gate pulses of the inverter circuit. The primary limitation of the PI controller arises from its linear design, which makes it incapable of efficiently managing non-linearities in the electrical grid network [12]. Therefore, more methods must be developed to optimally and dynamically modify the gain parameters for better performance. The basic mathematical equation of a PI controller can be represented as [11]:

$$x(t) = K_p e(t) + K_i \int e(t).dt \qquad (6)$$

3.2 Proposed Mountain Gazelle Optimiser (MGO)

3.2.1 General Theory

A species of Gazelle, the Mountain Gazelle, ascends from the Arabian Peninsula and its adjacent areas. In these areas, the population spread is significant, but the countable density is scarce [55]. The Robinia trees share a similar adaptation strategy with the mountain gazelle. With the increase in temperature during the later Holocene period, these animals get dispersed towards the Gazella bennett, a well-adapted place for the hot climate [56].

Being a territorial species, the vast distance splits their territory. Mother-offspring, young-male, and adult (bachelor) male herds are some groups they formed, where regular duels can be found, once the male turns adult. The challenge for males to sustain the climate is less violent than the female possession fights, and is more dramatic. Adult or mature males use their horns much less than immature males during fights. The span of food exploration can range over 120 km, where a mountain gazelle can run at 80 km/h for a stretch of hundreds of meters, which depicts their high speed, as illustrated in Fig.4

Fig.4. A Gazelle at high-speed crossing rocky altitudes

3.2.2 Mathematical Modelling

The Mountain Gazelle Optimiser, an algorithm inspired by the social conduct and day-to-day activities of a mountain gazelle, is derived from the patterns of social and group dynamics of a gazelle, thus forming an inspiration for the model [56]. The MGO algorithm operates depending on four critical factors in the animal's life: i) Single-male herds; ii) Mother-offspring herds; iii) Territorial Solitary males; and iv) Movement during the exploration of food [57]. MGO algorithm states: A gazelle (X_i), is part of any herd during the optimisation process, whereas a newborn can be from any herd except single male herds, where the males are young and immature. In the overall space, one-third of the exploration space is determined to be of minimal cost in contrast to other options for modelling [55].

Mother-offspring herds among the gazelles are the other solutions available in the entire space. With the termination of every cycle, strong individuals with a quality solution are preserved for the optimum solution [56, 58]. The lower-cost population is incorporated into the entire space, and the leftovers are treated as being over-aged. The ill gazelles are thus excluded from the space [55]. Using four mechanisms, exploration and exploitation stages are performed in parallel following the nature of the algorithm, which ensures the effective operation of the stages and enhances the likelihood of achieving the best solution and operation adhering to four mechanisms, as presented in Fig. 5 [56].

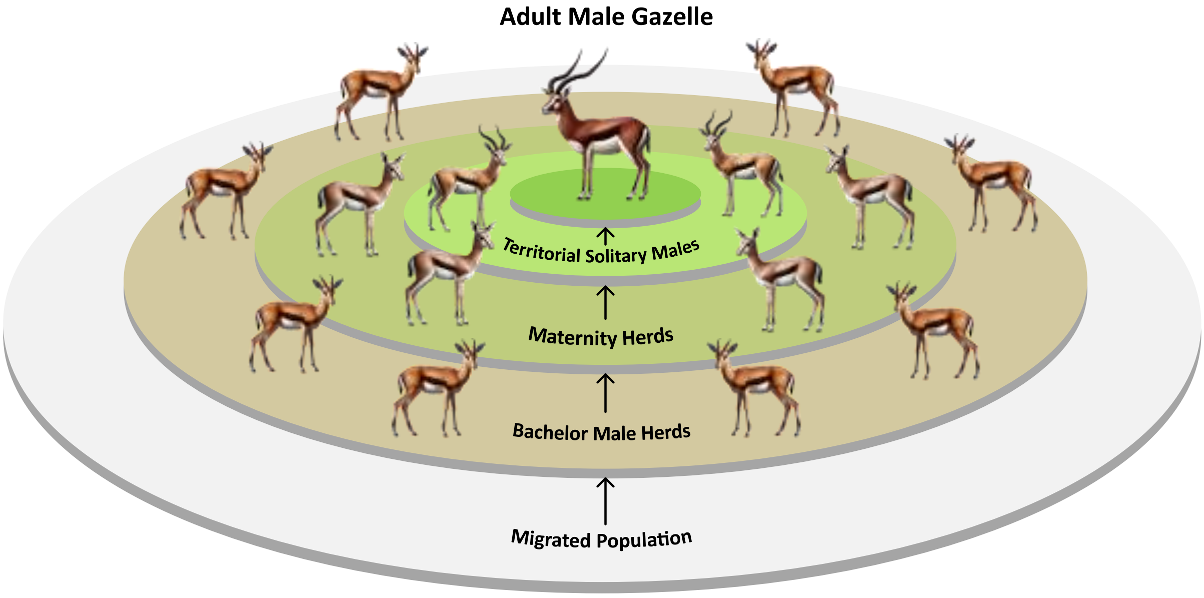

Fig.5. Mountain Gazelles Optimiser Process

3.2.2.1 Territorial Solitary Males

With maturity, strength, and adulthood, a male gazelle builds its solitary territory with great distances separating them. Duels between these adult males occur due to territory succession or female possession, where the young one tries to capture the territory or the female, and adults safeguard their surroundings [57].

The model of an adult male's territory can be mathematically written as [14]:

$$TSM = male_{gazelle} - \left|(ri_1 * BH - ri_2 * X(t)) \times F\right| \times Cof_r \quad (7)$$

Where, $male_{gazelle}$ is the position vector of the adult male (quality solution). ri_1 and ri_2 represents some randomly selected numbers, such as 1 or 2.

BH, F, Cof_r depicts the coefficient vector of the male herd (young), dimensions used, and random vector updated to every repetition, thus used to amplify the exploration capability respectively.

$$BH = X_{ra} * [r_1] + M_{pr} \times [r_2],\ r_a = \left\{\left[\frac{N}{3}\right] \ldots.. N\right\} \quad (8)$$

Here, X_{ra} represents the young male's random solution for the 'r_a' interval.

N represents the entire gazelle population, and $\left[\frac{N}{3}\right]$ depicts the average gazelle population.

r_1 and r_2, depicts the randomly selected values of either 0 or 1.

$$F = N_1(D) \times \exp\left(2 - iter \times \left(\frac{2}{MaxIter}\right)\right) \quad (9)$$

Here, N_1 represents the randomly selected number from the standard deviation.

exp being the exponential function. $iter$ and $MaxIter$ are the current and maximum allowed

iterations, respectively.

$$Cof_i = \begin{cases} (a+1) + (r_3) \\ (a) * N_2(D) \\ r_4(D) \\ N_3(D) * N_4(D)^2 * \cos(((r_4) * 2) * N_3(D)) \end{cases} \quad (10)$$

Here, r_3 and r_4 represents the randomly selected number, 0 or 1.

$N_2, N_3, and\ N_4$ represent the dimensions, in the normal range. cos being the cosine function.

a is the amplitude of Cof vector variation, which can be calculated as,

$$a = -1 + Iter \times \left(\frac{-1}{MaxIter}\right) \quad (11)$$

3.2.2.2 Maternity/ Mother-offspring herds

In the life of the mountain gazelle, maternity herds play a vital role in reproduction. They help in maintaining the cycle of births and production, which can be written as:

$$MH = (BH + Cof_{1,r}) + (ri_3 \times male_{gazelle} - ri_4 \times X_{rand}) \times Cof_{1,r} \quad (12)$$

Here, $Cof_{2,r}, Cof_{3,r}$ are the random coefficient vectors, ri_3, ri_4 are randomly selected integers of value 1 or 2. X_{rand} represents a random gazelle's position vector [55].

3.2.2.3 Single male herds

With time, the newborns grow, become strong and mature, fight and build their territories, and thus possess female gazelles. These duels are often too violent. A Mountain Gazelle's behaviour can be formulated as:

$$BMH = (X(t) - D) + (ri_5 \times male_{gazelle} - ri_6 \times BH) \times Cof_r \quad (13)$$

Here, $X(t)$ represents the position vector. ri_5 and ri_6 The randomly selected integers are 1 or 2.

D can be mathematically formulated as:

$$D = (|X(t)| + |male_{gazelle}|) \times (2 \times r_6 - 1) \quad (14)$$

Here, r_6 is a randomly selected number between 0 and 1.

3.2.2.4 Movement during the exploration of food

Exploring food, the mountain gazelles traverse considerably as shown in Fig.6. Gazelles can run at higher speeds and jump high. This behaviour can be formulated as [55]:

$$MSF = (ub - lb) \times r_7 + lb \quad (15)$$

Here, ub, lb represent the upper and lower ranges. r_7 is an arbitrarily chosen number between 0 and 1.

Fig.6. Herd of Gazelles in search of food

Territorial Solitary Males (TSM), Male Herd (MH), Coefficient vector of the bachelor male herd (BMH), and Movement during the search for food (MSF) formulas are employed to reproduce the entire population of the gazelles. A single replication occurs in each generation, and a new era is added to space. At the end of each era, the gazelles are organised in an ascending order [56]. High-quality best gazelles with promising solutions and cheaper prices are conserved. Rest, weak and old gazelles are excluded.

3.2.3 Complexity of the MGO Algorithm

Primary influencing factors are initialisation, fitness assessment, and gazelle update [55].

$$\mathrm{CC} = O(T \times N \times D \times 4) \quad (16)$$

Here, the Computational cost for initialisation is represented as O, and N is the total gazelle population. D refers to the dimension and T is the maximum iterations.

Upon evaluation of the cost function, the Computational Complexity (CC) for Mountain Gazelle Optimiser comes out as:

$$\mathrm{CC} = O(T \times N \times 4) \times O(f(p)) \quad (17)$$

3.2.4 Exploration, Exploitation, and Convergence

Four Four different mechanisms optimise every searching factor and number of iterations. Every mechanism has its characteristics, and every tool improves the algorithm's performance. Every mechanism uses coefficient vectors to bring about movements in the search agents. Four operations are applied in the MGO on each search agent, resulting in search agents moving through a population size ($\boldsymbol{N}$=30) and maximum iteration ($\boldsymbol{T}$=100) toward the solution. Exploration and exploitation phases run parallel, searching the problem space, avoiding an optimal local trap. At every optimisation step, the exploration agents move toward a high-quality solution, ensuring all agents gather the current best solutions in a single optimal point. The symbols and their corresponding meaning used in the MGO method have been presented in Table I.

.

Table I. Symbol and meaning of terms used in the MGO method.

Symbol	Meaning	Symbol	Meaning
TSM	Territorial Solitary Males	X_{rand}	Random gazelle's position vector
$male_{gazelle}$	Position vector of the adult male	BMH	Bachelor Male Herd
$ri_1, ri_2..ri_6$	Randomly selected numbers, 1 or 2	$X(t)$	Position vector
BH	Coefficient vector of the bachelor male herd	MSF	Movement during the search for food
X_{ra}	Young male's random solution for 'r-a' interval.	ub	Upper range
F	dimensions used	lb	Lower range
Cof_r	Random vector updated to every repetition	CC	Computational complexity
N	entire gazelle population	O	Computational cost
$\left[\frac{N}{3}\right]$	Average gazelle population	T	max. iterations
$r_1, r_2 \ldots r_7$	randomly selected values of either 0 or 1.	D	dimension
$N_1(D)$	Randomly selected number from the standard deviation	MGO	Mountain Gazelle Optimiser
exp	exponential function	MH	Maternity Herds
$Iter$, $MaxIter$	Current and Maximum allowed Iteration	a	The amplitude of the Cof vector variation

3.3 Pseudocode of MGO

Step 1. Initialisation- **population size**, **maximum iterations**

Step 2. Calculate the **gazelle's fitness**

Step 3. Apply loops to calculate and find a solution.

While (stop criteria don't meet) do

for each Gazelle (X_i)) do

Evaluate **TSM** as of **Eq. (7)**

Evaluate **MH** as of **Eq. (12)**

Evaluate **BMH** as of **Eq. (13)**

Evaluate **MSF** as of **Eq. (15)**

Assess the effectiveness of each step, thereby implementing it within the habitat.

end for.

Step 4. Organise the entire space **ascendingly**.

Step 5. The **best** individual gazelle is found and added.

Step 6. Conserve the best gazelles from the entire population and **remove** the weak and old.

Step 7. End loop, Return the **best solution**

end while

Return solution.

3.4 Flowchart of MGO

The complete process involved in the MGO strategy has been briefly represented using a flowchart as depicted in Fig.7 for easy understanding by the readers.

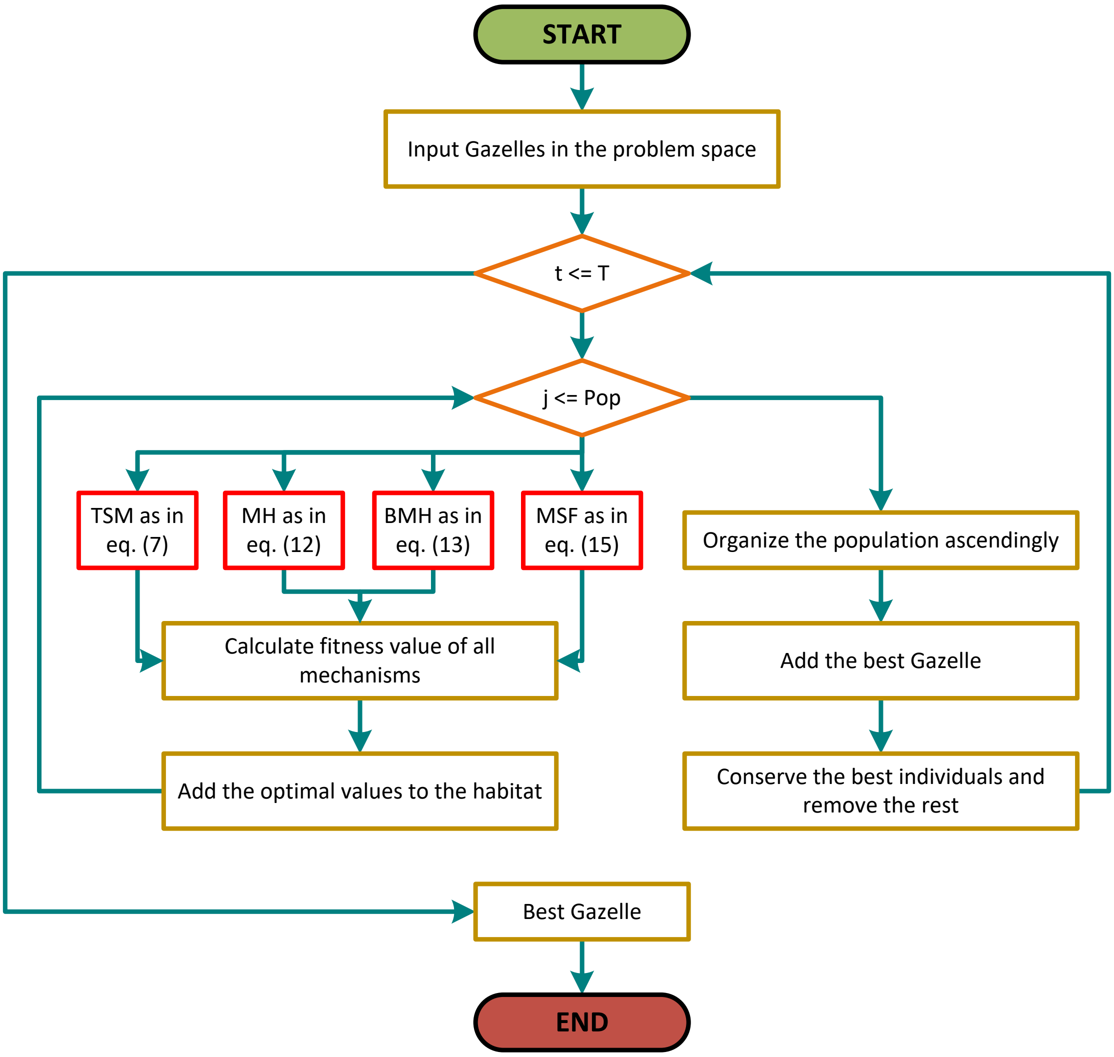

Fig.7. The Flowchart for MGO Algorithm.

3.5. Rationale for Choosing Mountain Gazelle Optimizer (MGO)

The Mountain Gazelle Optimizer (MGO) was selected for this study due to its demonstrated ability to balance exploration and exploitation effectively, which is essential for avoiding local minima during PI controller tuning in complex, nonlinear systems like SAPF-based microgrids. Its derivative-free nature makes it well-suited to problems where gradient information is challenging to obtain. MGO's fast convergence and computational simplicity also make it attractive for engineering applications. Although this work focuses on the feasibility and performance of MGO for SAPF PI tuning, a detailed comparison with other optimization algorithms is planned for future work.

3.6 Application of MGO Algorithm for Dynamic and Optimum Tuning of the Gain Parameters of the PI Controller

To ensure the optimum performance of the hybrid renewable energy system (HRES) comprising photovoltaic (PV) panels, fuel cells (FC), and batteries, the Mountain Gazelle Optimiser (MGO) approach has been utilised in this research work. MGO helps in finding optimal and dynamic gain values of the PI parameters (K_p and K_i) which can robustly respond to any PQ disturbances in the MG system. Here, minimisation of the three objective functions ($Ob\ Fn$) is considered the optimisation problem in Eq. (17-19). It uses the Integral Time Absolute Error (ITAE) standard. Fig.8(a), Fig.8(b) and Fig.8(c) demonstrate the framework for the inverter's duty cycle generation with the MGO method for PV, FC and battery, respectively. The following are the three objective functions:

$$Ob\ Fn_1 = \int_0^t (\mathrm{ER_1(t)})^2\, \mathrm{dt} \tag{17}$$

$$Ob\ Fn_2 = \int_0^t (\mathrm{ER_2(t)})^2\, \mathrm{dt} \tag{18}$$

$$Ob\ Fn_3 = \int_0^t (\mathrm{ER_3(t)})^2\, \mathrm{dt} \tag{19}$$

Where,

$$ER_1(t) = \Delta P_{PV} = P_{PV} - P_{LOAD} \quad (20)$$

$$ER_2(t) = \Delta P_{FC} = P_{FC} - P_{LOAD} \quad (21)$$

$$ER_3(t) = \Delta\, SOC_{Bat} = SOC_{Bat\_ref} - SOC_{Bat\_load} \quad (22)$$

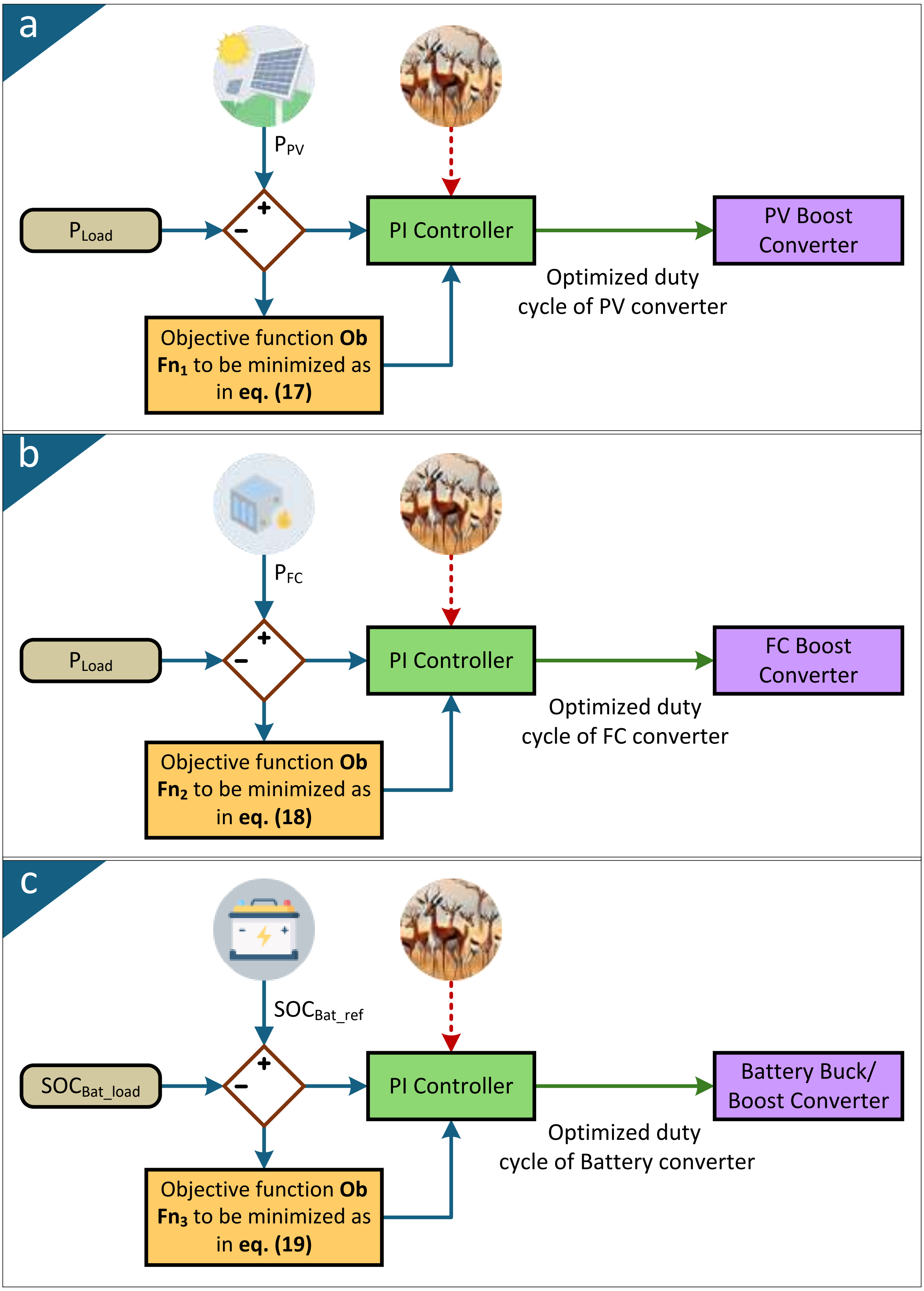

Fig.8. Framework for inverter's duty cycle generation with MGO method (a) PV, (b) FC and (c) Battery.

4. MATLAB/Simulink Architecture with Result Analysis

4.1 Description of Simulink Architecture

This study investigation focuses on a hybrid renewable energy system (HRES) that consists of battery-based distributed generation units, fuel cells, and photovoltaic (PV) distributed generation units to form a microgrid (MG) system. A SAPF is also employed to bring about harmonic mitigation, reactive power compensation, power factor correction, voltage regulation, load balancing, reduction of oscillations and an overall increase in the system reliability on the onset of PQ faults. Power electronic interfaces (PEIs) have been used, including DC-DC buck/boost converters (for the battery), DC-DC boost converters (for PV/FC), and DC-AC converters. The MATLAB/Simulink architecture was employed to build each component of the MG system. Numerous simulated responses of the MG system at the source and load end were analysed for both the conventional and suggested controller approaches. A block diagrammatic representation of the SAPF-MGO system with different controllers under investigation is shown in Fig.9 below. The SAPF model designed and undertaken for the study is shown in Fig.10. Table III in the Appendix has the values for each MG unit undertaken for the study.

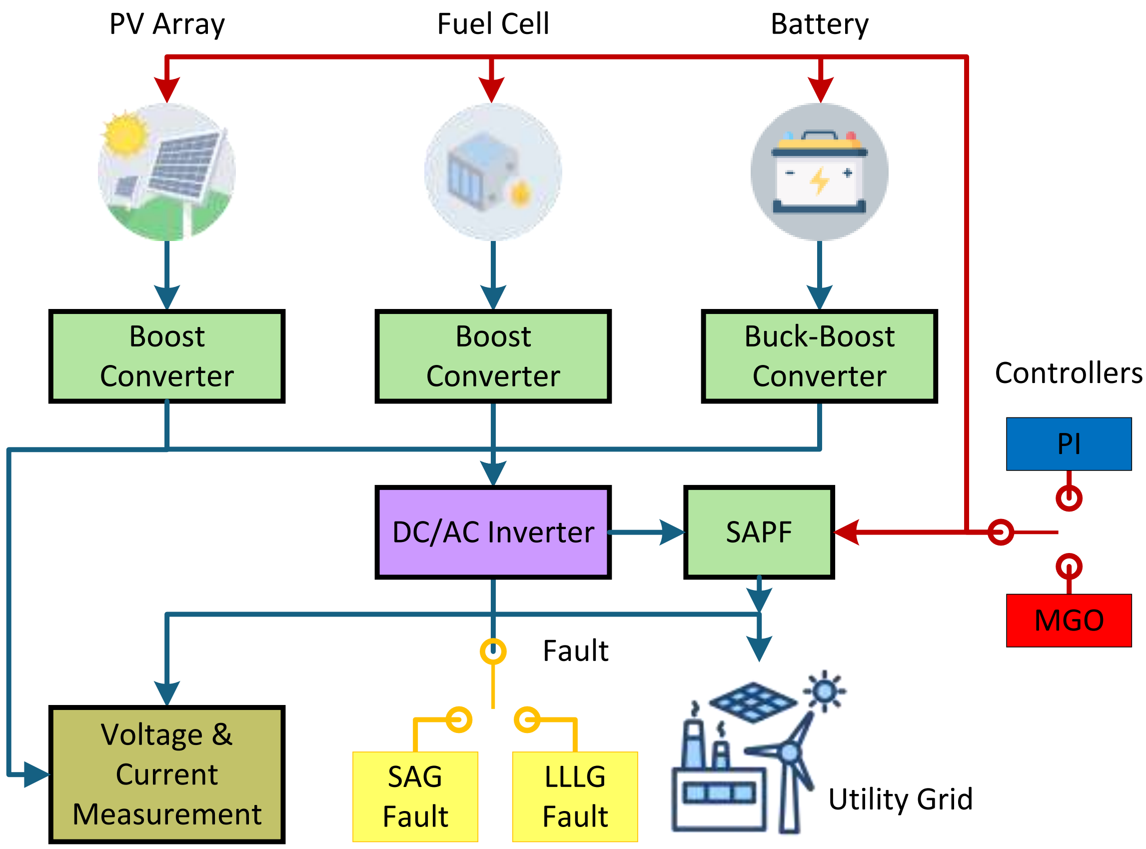

Fig.9. HRES-based MG architecture in MATLAB/Simulink Architecture

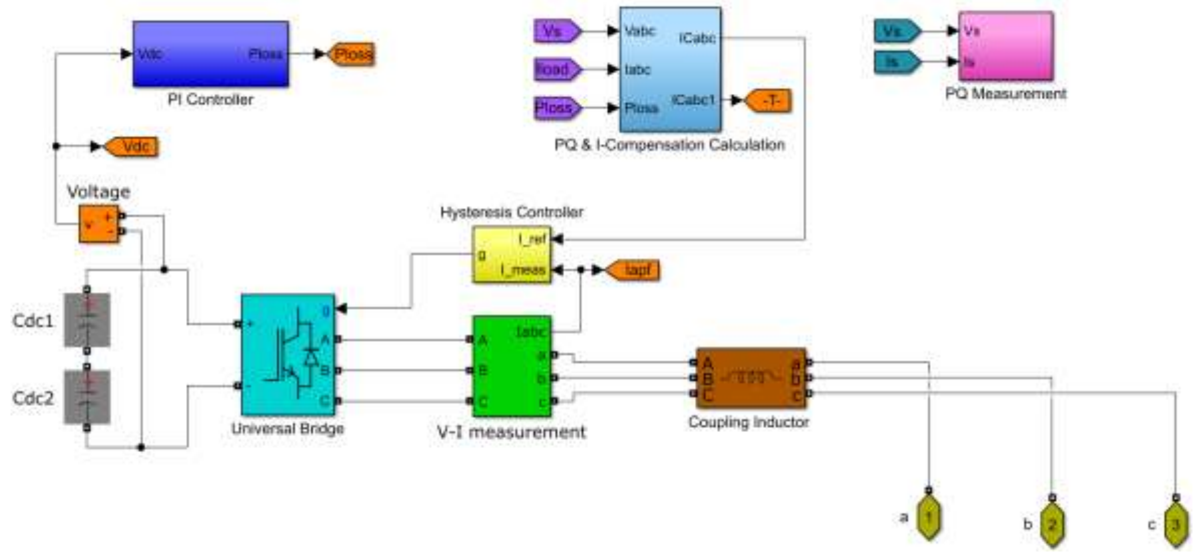

Fig.10. SAPF model designed and undertaken for the study

4.2 Discussion of Simulation Outcomes

The effectiveness evaluation of the HRES-based microgrid MG was carried out with a critical analysis of the results and was broadly presented in two sections: 1) HRES proficiency on the supply side and 2) HRES proficiency on the grid side of the MG system subjected to PQ faults.

4.2.1 Supply Side Responses (PV, FC, Battery and SAPF)

The functionality and characteristics of the HRES, which comprises the PV, FC, and battery (at the supply end) and the compensating current provided by SAPF, are presented in this portion of the article. The responses of the suggested MGO-tuned PI controller and traditional PI controller have been studied meticulously, and detailed findings have been discussed. The output characteristics of the supply side, namely PV, Fuel Cell and Battery, have been depicted in Fig.11-15, Fig.16-18 and Fig.19-22, respectively.

PV Power Vs Voltage and PV Current Vs Voltage obtained from the proposed MGO tuned PI controller are indicated in Fig.11 and Fig.12, respectively. A comparative illustration between suggested MGO-based PI and traditional PI for PV voltage, PV current and PV power output responses has been shown in Figs. 13 to 15, respectively. The FC voltage, FC current and FC responses obtained from MGO-PI and PI are portrayed in Figs. 16 to 19, systematically. Battery's voltage, current, power, and State of Charge (SoC) are presented in Figs. 20 to 22, in order. It is evident from the graphical results that the PI controller tuned by the proposed MGO strategy exhibits superior performance with respect to the customary PI controller, pertaining to improved stability, lower distortions, augmented system-wide dynamic behaviour, and better efficiency. The SAPF compensating current for Phase-A for the proposed and conventional PI method is represented in Fig.23. The result indicates that the MGO-tuned PI possesses advanced capability of providing compensating current as compared to the traditional PI controller.

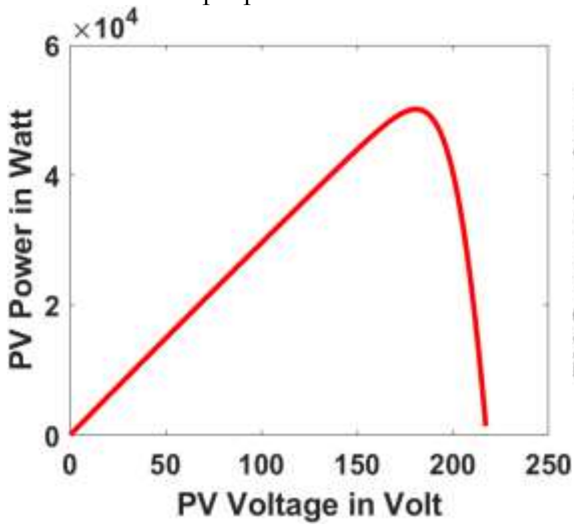

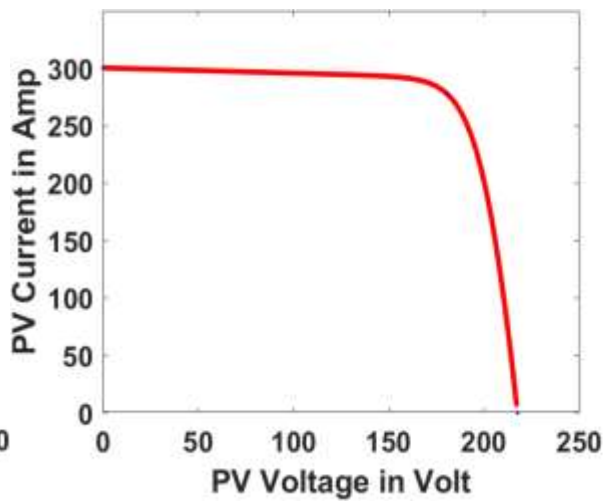

Fig.11. PV Power Vs PV Voltage

Fig.12. PV Current Vs PV Voltage

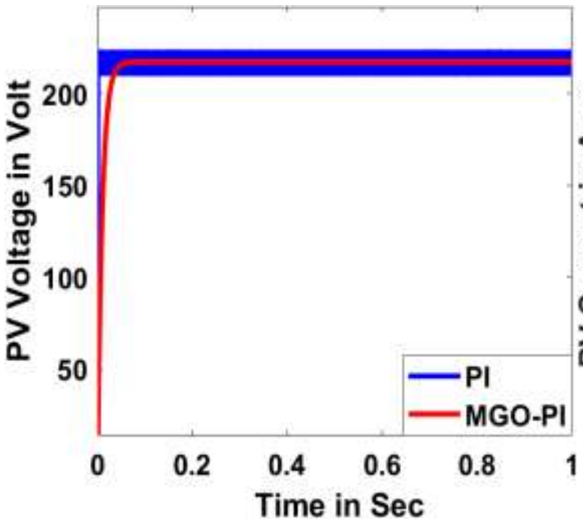

Fig.13. PV Voltage Vs Time

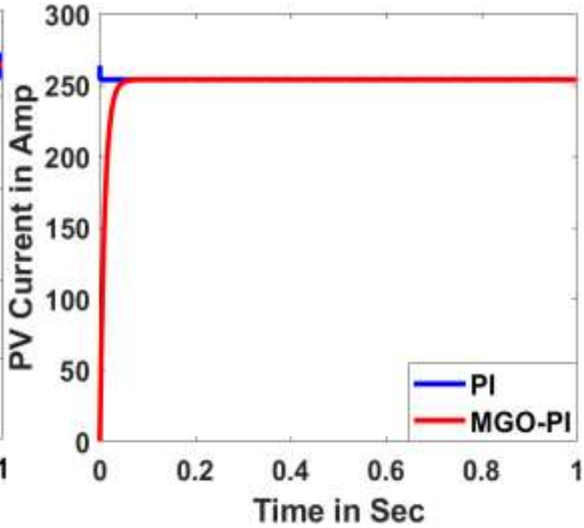

Fig.14. PV Current Vs Time

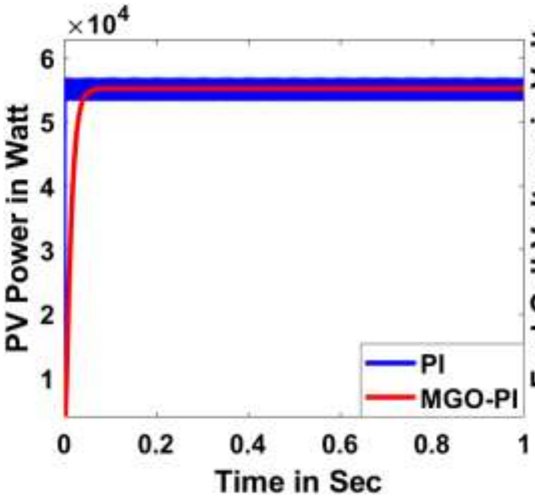

Fig.15. PV Power Vs Time

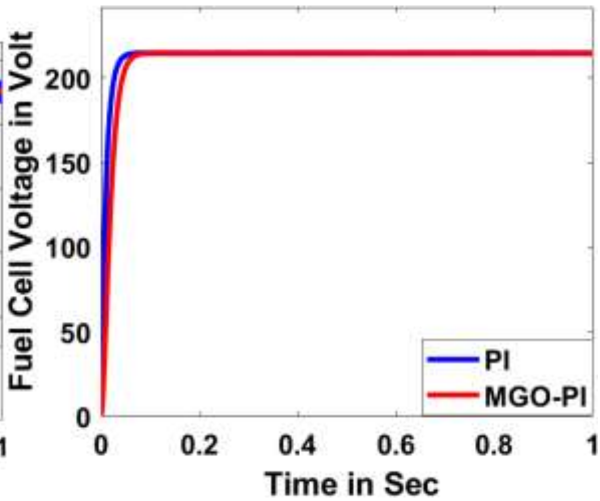

Fig.16. FC Voltage Vs Time

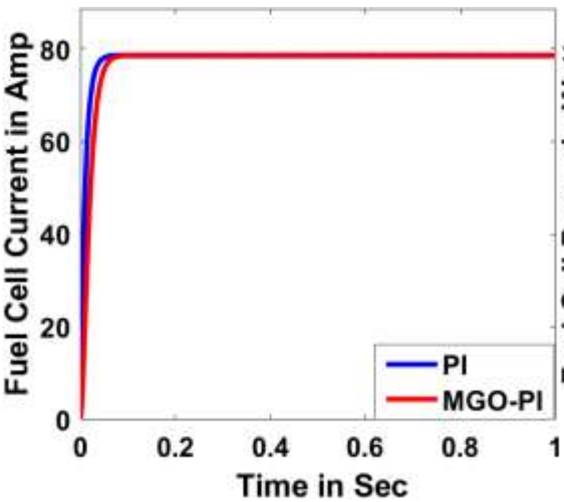

Fig.17. FC Current Vs Time

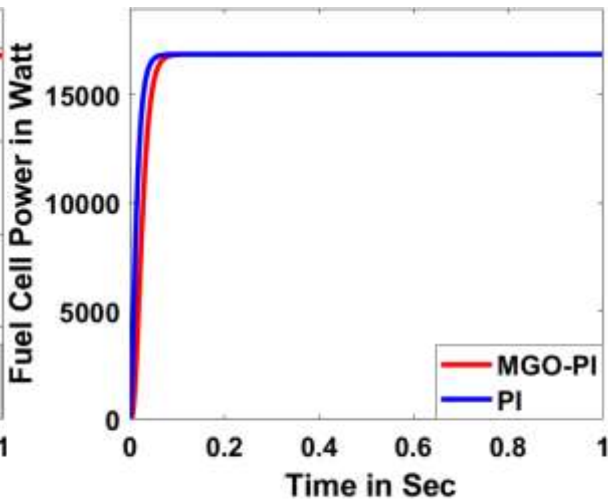

Fig.18. FC Power Vs Time

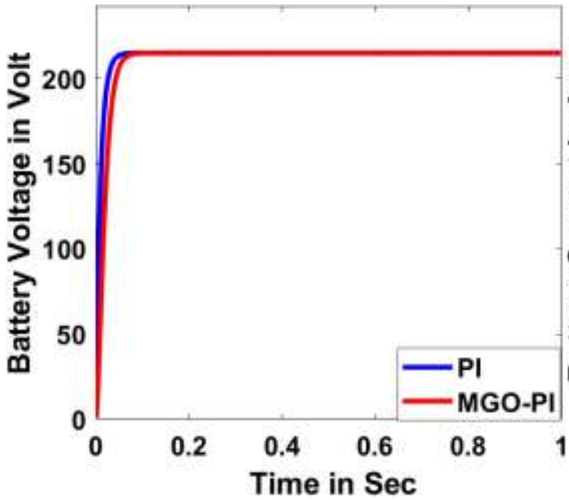

Fig.19. Battery Voltage Vs Time

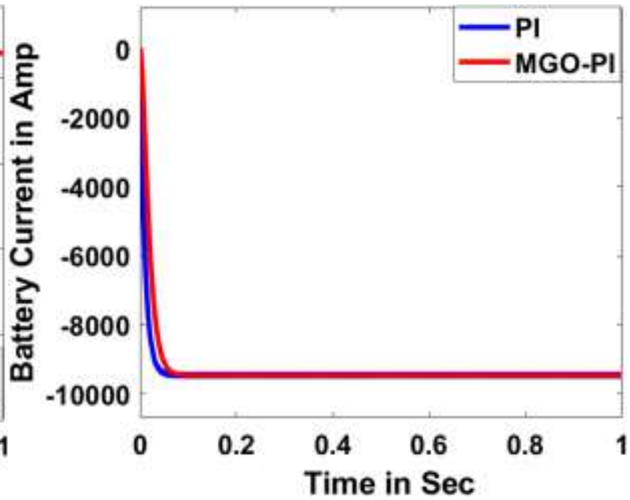

Fig.20. Battery Current Vs Time

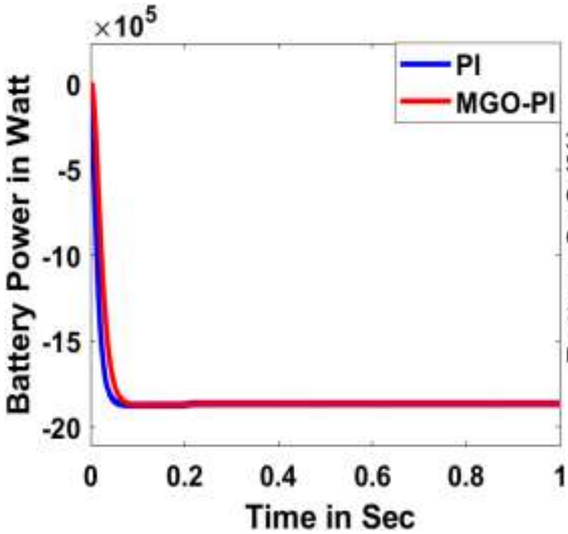

Fig.21. Battery Power Vs Time

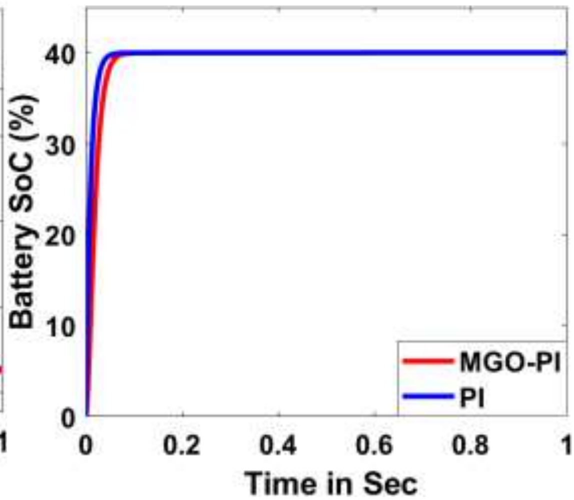

Fig.22. Battery SoC Vs Time

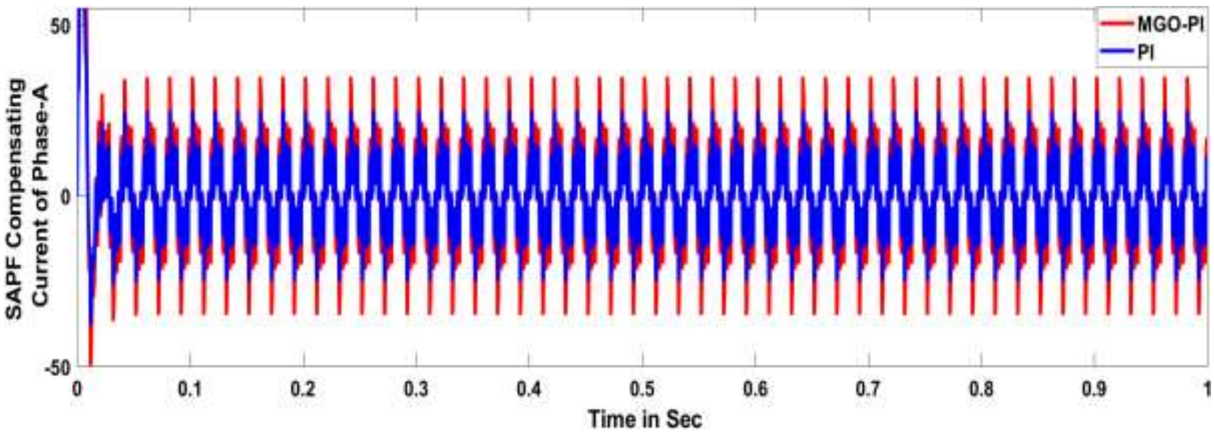

Fig.23. SAPF Compensating Current for Phase-A

4.2.2 Grid Side Responses subjected to different PQ faults

Performance metrics of the system and responses of the hybrid MG unit in the grid-connected mode of working have been thoroughly examined in this section. To justify the resilience and efficacy of the suggested MGO-tuned PI controller over the conventional PI technique, the MG system has been deliberately led to 2 types of severe PQ faults from 0.4 Sec to 0.6 Sec: 1) SAG fault and 2) LLG fault. An in-depth outline of the techniques adopted to create the above faults has also been vividly explained. The simulation responses for varied system characteristics (like DC-link voltage, voltage deviation, terminal voltage, power factor, frequency, grid active power, THD, grid apparent power, grid reactive power, grid's voltage without SAPF, grid phase voltage with SAPF, grid's current without SAPF and grid's phase current with SAPF) of both the fault cases have been observed and a detailed comparative analysis of MGO tuned PI controller and traditional PI controller have been exhibited.

After a critical examination and assessment of the simulation responses, it was found that the PI controller, which was optimised using the suggested MGO method, considerably improved system efficiency, reliability, and power quality compared to traditional PI controllers. The MGO-tuned PI method excelled over the conventional PI methods in terms of predominant mitigation of harmonics, better control of active, reactive as well as apparent power, enhanced power factor, lowered deviation in voltage, sustaining voltage at terminal, DC link voltage, grid voltage and current (with SAPF) nearly steady even on the onset of the power quality disturbances.

4.2.2.1 SAG Fault

The SAG fault has been generated by introducing a 3-ϕ LLG fault. Various system dynamic responses of the MGO-tuned PI and traditional PI methods such as voltage at DC-link, voltage at terminal, deviation in voltage, frequency, power factor, THD, grid's active power, grid's reactive power, grid's apparent power, grid voltage without SAPF, grid phase voltage with SAPF, grid current without SAPF and grid current with SAPF have been found in simulation environment and shown in Fig.24 (a), (b), (c), (d), (e), (f), (g), (h), (i), (j), (k), (l) and (m) respectively.

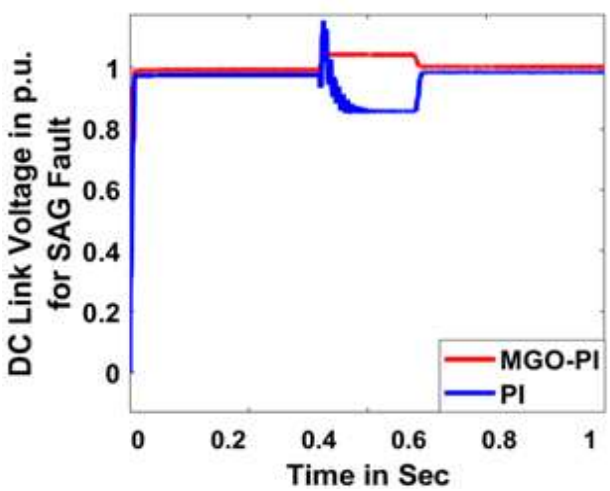

Fig.24(a).Voltage at DC Link for SAG

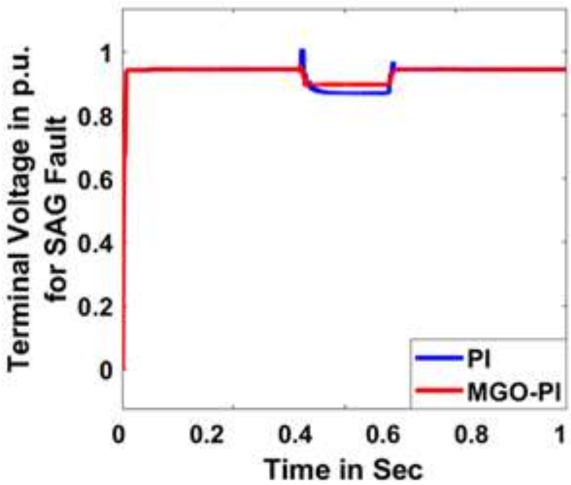

Fig.24(b).Voltage at Terminal for SAG

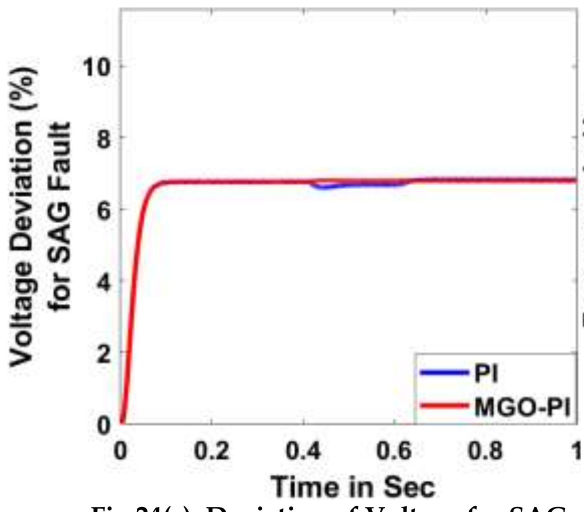

Fig.24(c). Deviation of Voltage for SAG

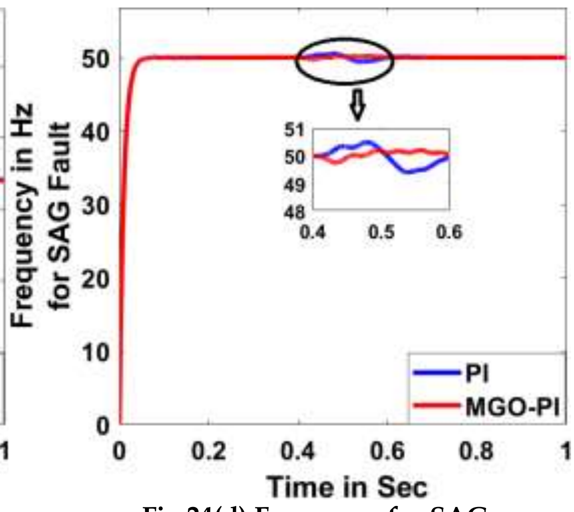

Fig.24(d).Frequency for SAG

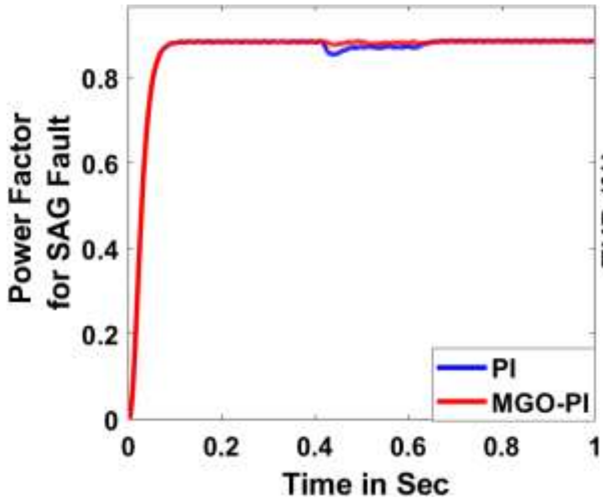

Fig.24(e).Power Factor for SAG

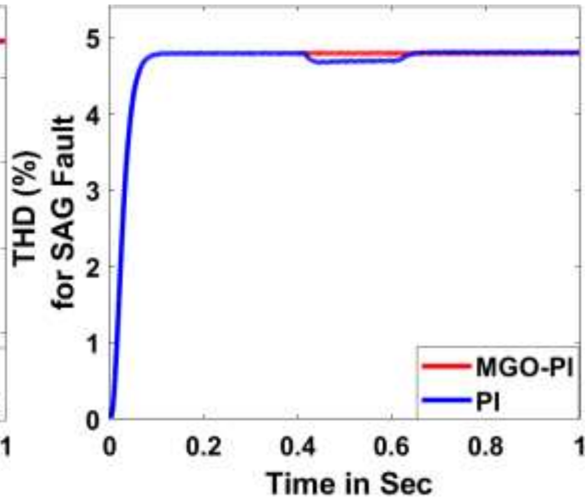

Fig.24(f).THD (%) for SAG

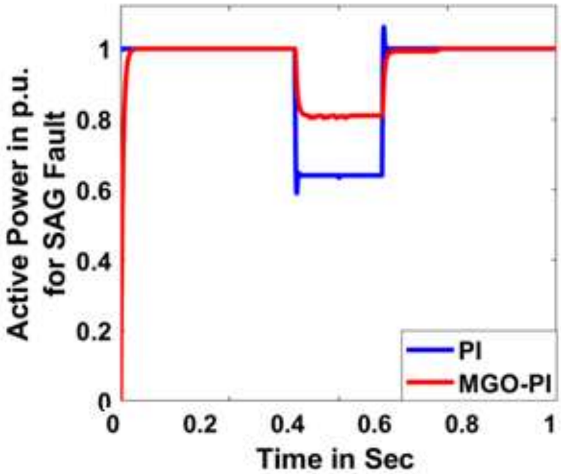

Fig.24(g).Active Power for SAG

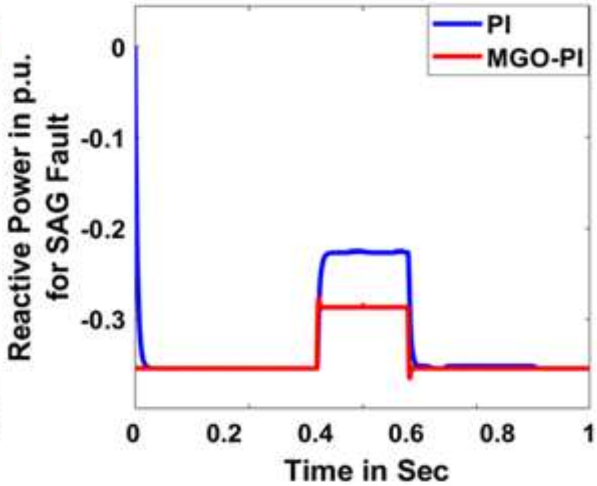

Fig.24(h).Reactive Power for SAG

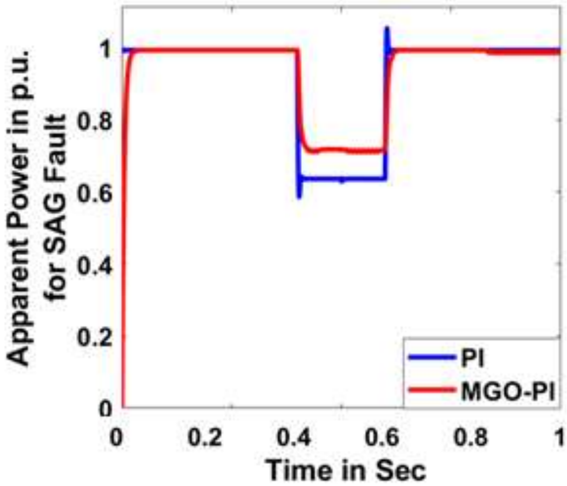

Fig.24(i).Apparent Power for SAG

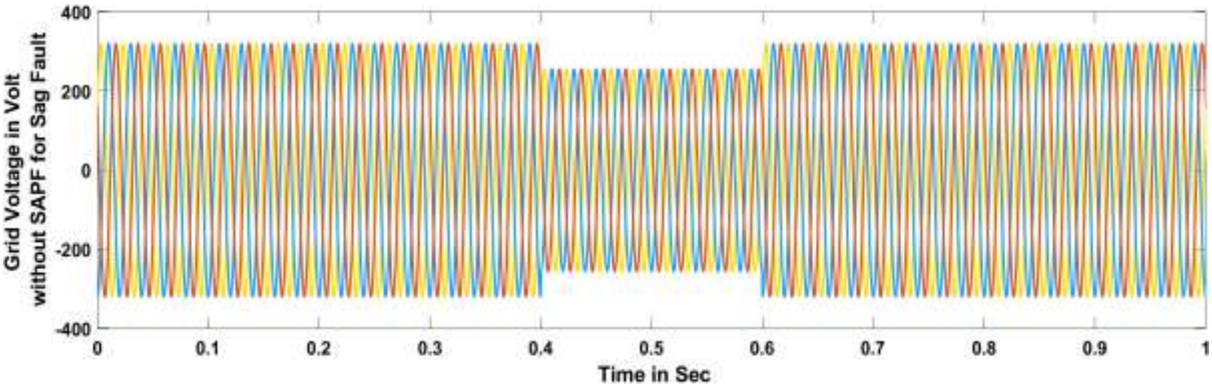

Fig.24(j).Grid voltage in Volts without SAPF for SAG

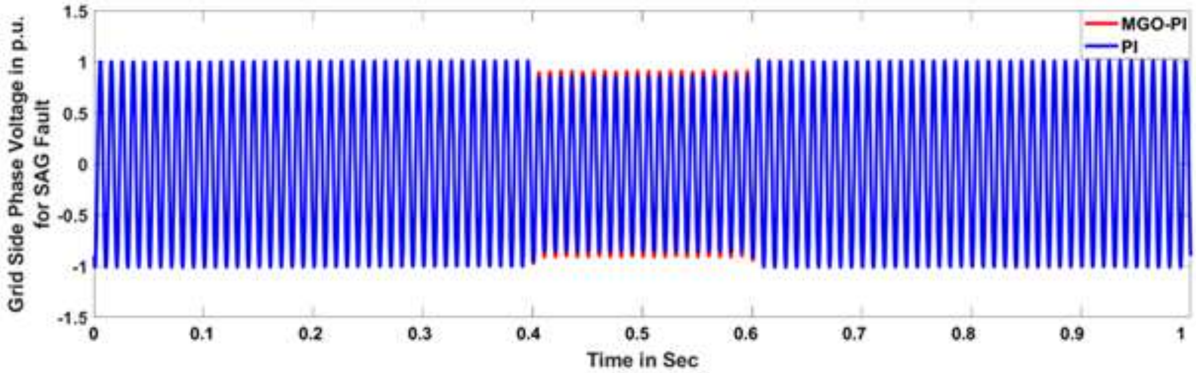

Fig.24(k). Grid side phase Voltage in p.u. for SAG

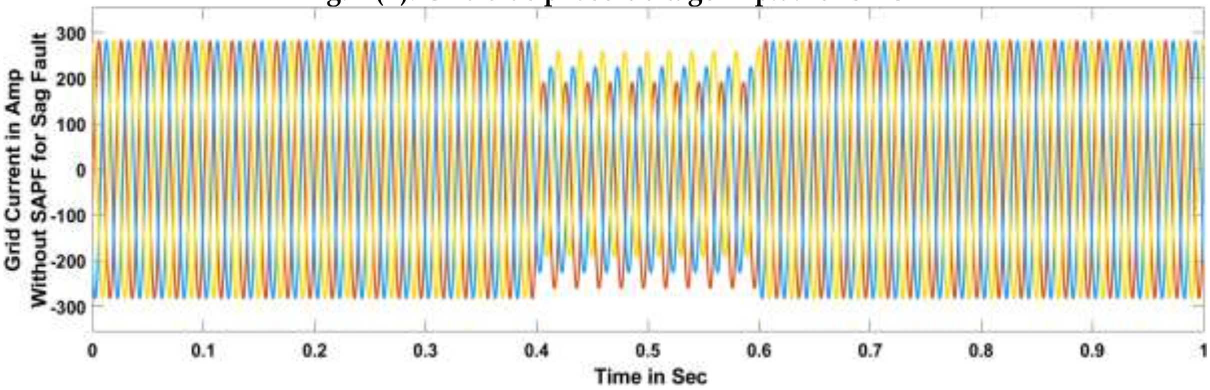

Fig.24(l). Grid current in Amp without SAPF for SAG

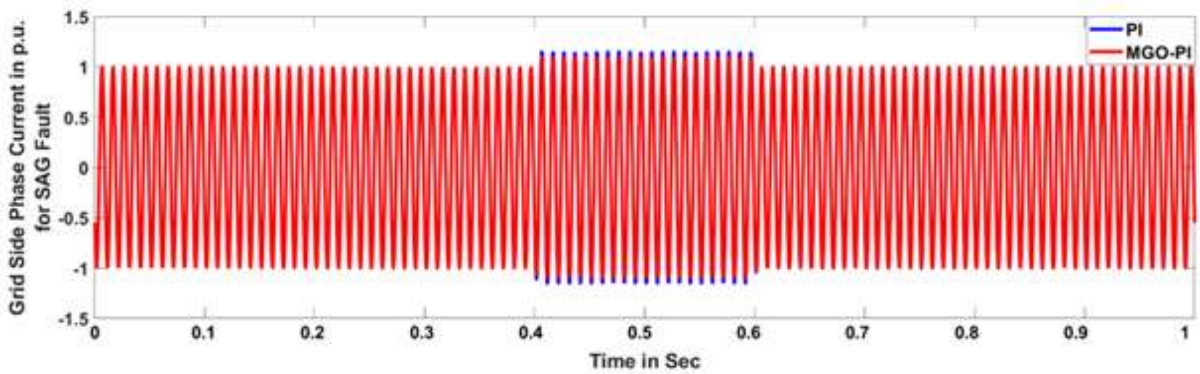

Fig.24(m). Grid side phase Current in p.u. for SAG

4.2.2.2 LLG Fault

An LLG fault has been created by short-circuiting the two lines and the ground. Fig.25 (a), (b), (c), (d), (e), (f), (g), (h), (i), (j), (k), (l) and (m) depicts a comparative response such as voltage at DC-link, voltage at terminal, deviation in voltage, frequency, power factor, THD, grid's active power, grid's reactive power, grid's apparent power, grid voltage without SAPF, grid phase voltage with SAPF, grid current without SAPF and grid current with SAPF systematically for MGO tuned PI and conventional PI techniques.

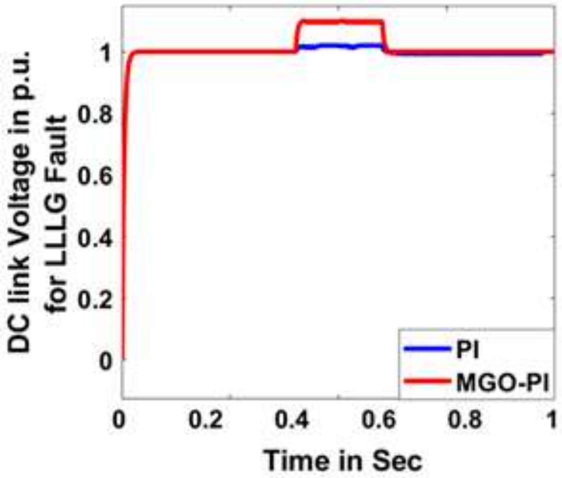

Fig.25(a).Voltage at DC Link for SAG

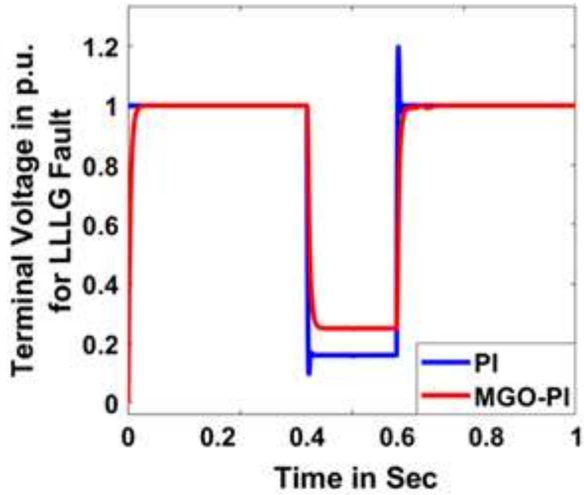

Fig.25(b).Voltage at Terminal for SAG

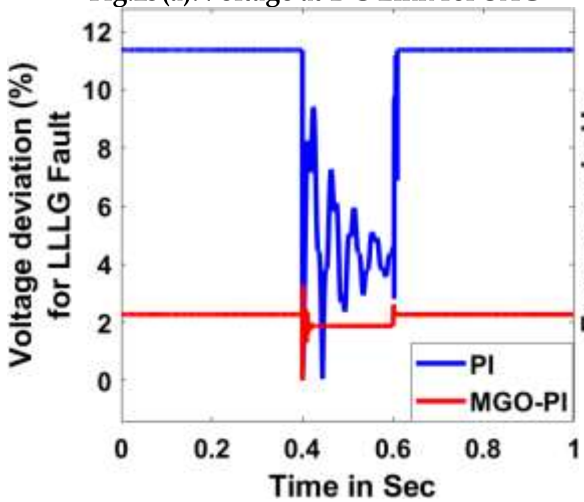

Fig.25(c). Deviation of Voltage for LLG

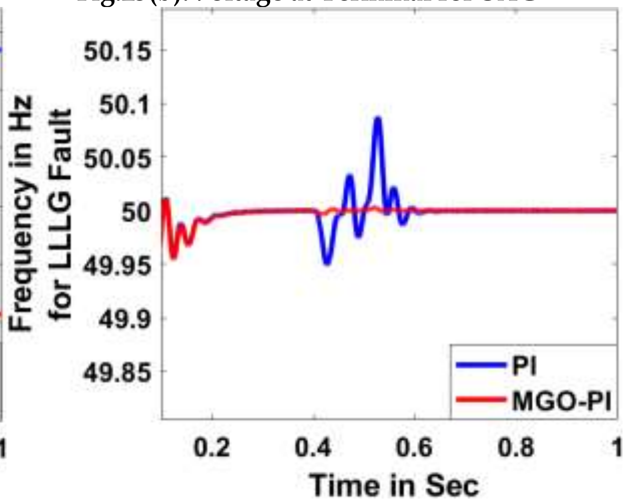

Fig.25(d).Frequency for LLG

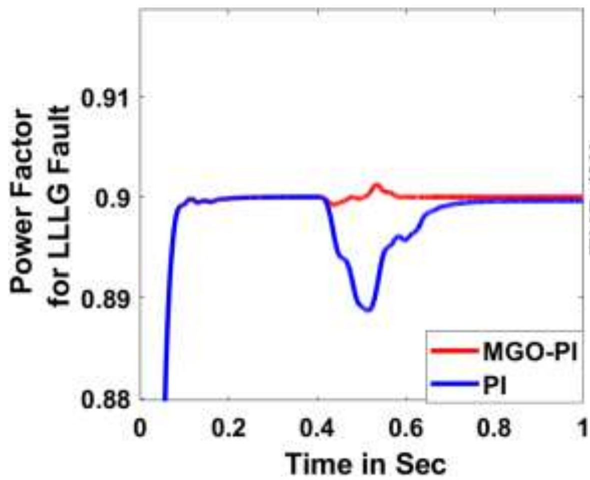

Fig.25(e).Power Factor for LLG

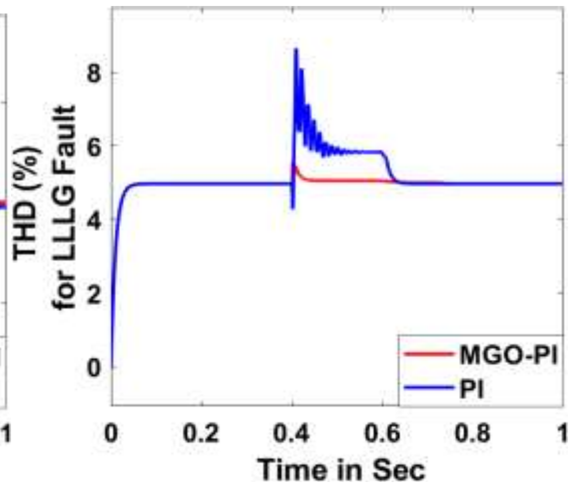

Fig.25(f).THD (%) for LLG

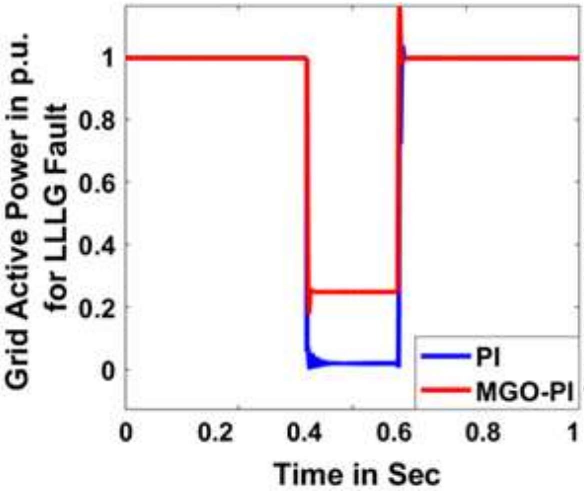

Fig.25(g).Active Power for LLG

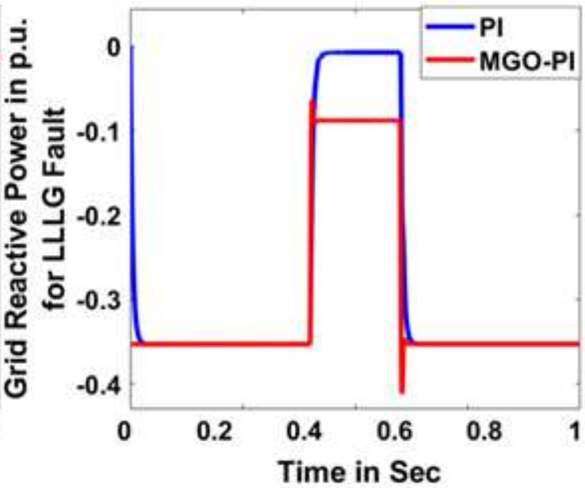

Fig.25(h).Reactive Power for LLG

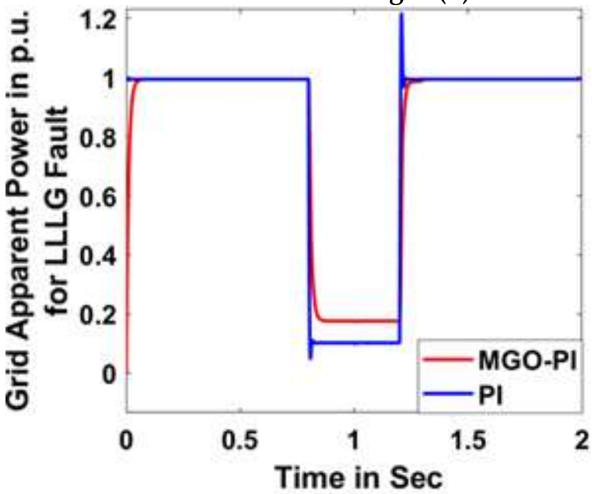

Fig.25(i).Apparent Power for LLG

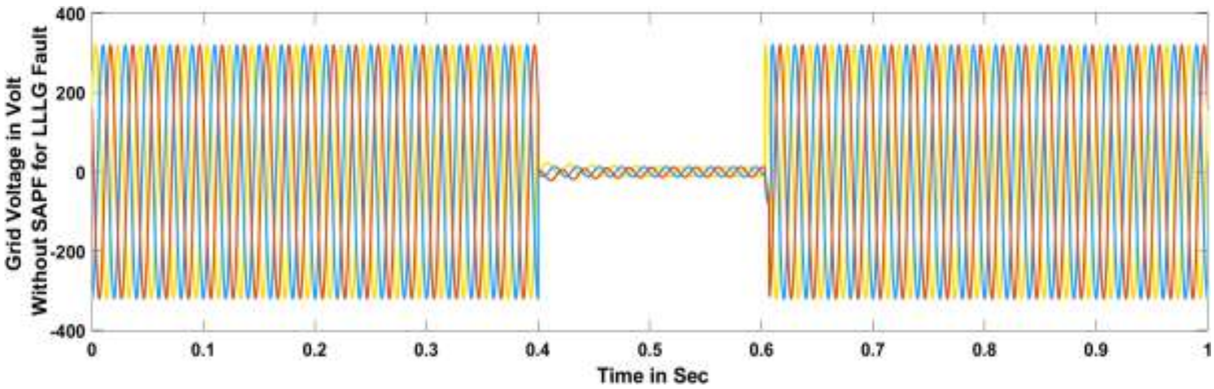

Fig.25(j).Grid Voltage in Volts without SAPF for LLG

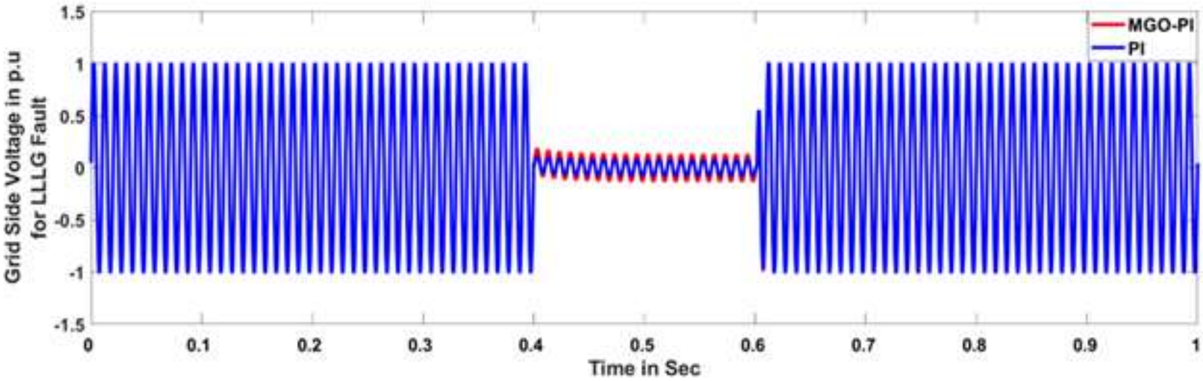

Fig.25(k). Grid Phase Voltage in p.u. with SAPF for LLG

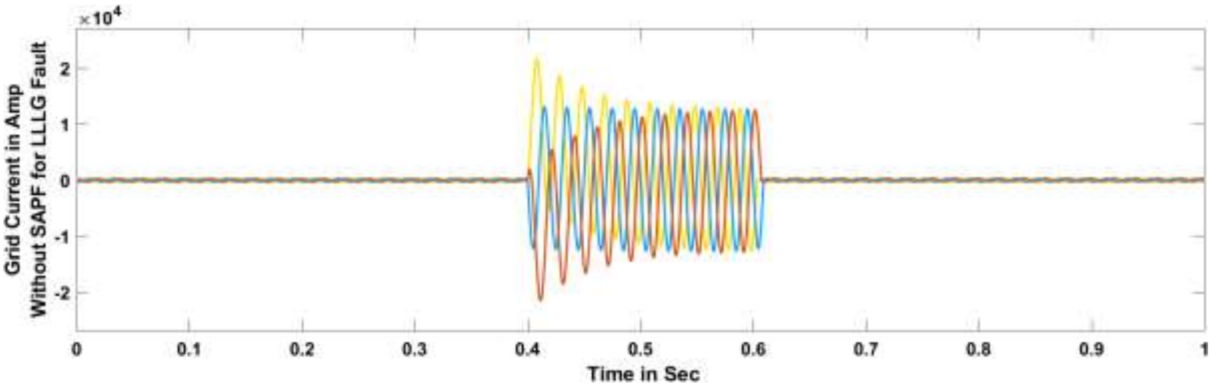

Fig.25(l). Grid Current without SAPF for LLG

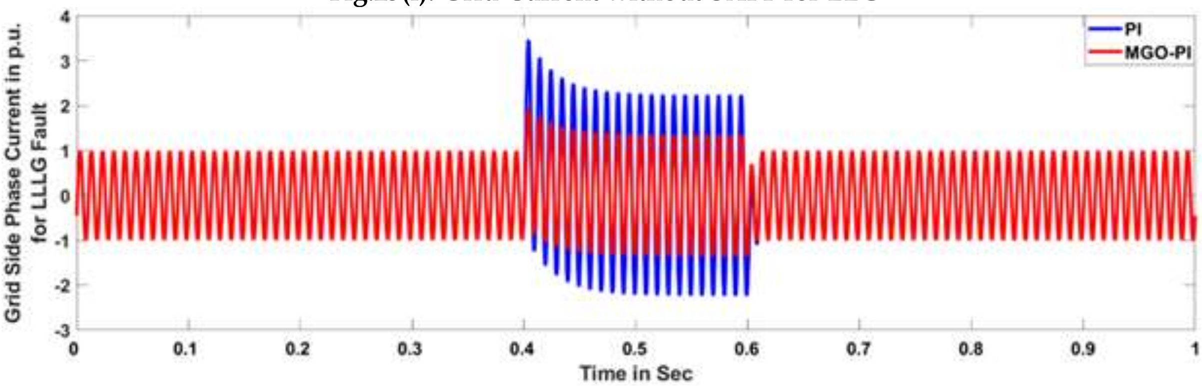

Fig.25(m). Grid Phase Current with SAPF for LLG

THD ANALYSIS

A detailed THD analysis for both grid voltage and grid current has been conducted to evaluate the harmonic mitigation capability of the proposed MGO-PI controller. The corresponding numerical values under SAG and LLG fault conditions are presented in Table II, while the graphical representations are shown in Figures 26(a) to 26(d). These results demonstrate the significant reduction in THD achieved by the proposed approach compared to the system without SAPF and with the conventional PI controller, confirming the superior performance of the MGO-PI.

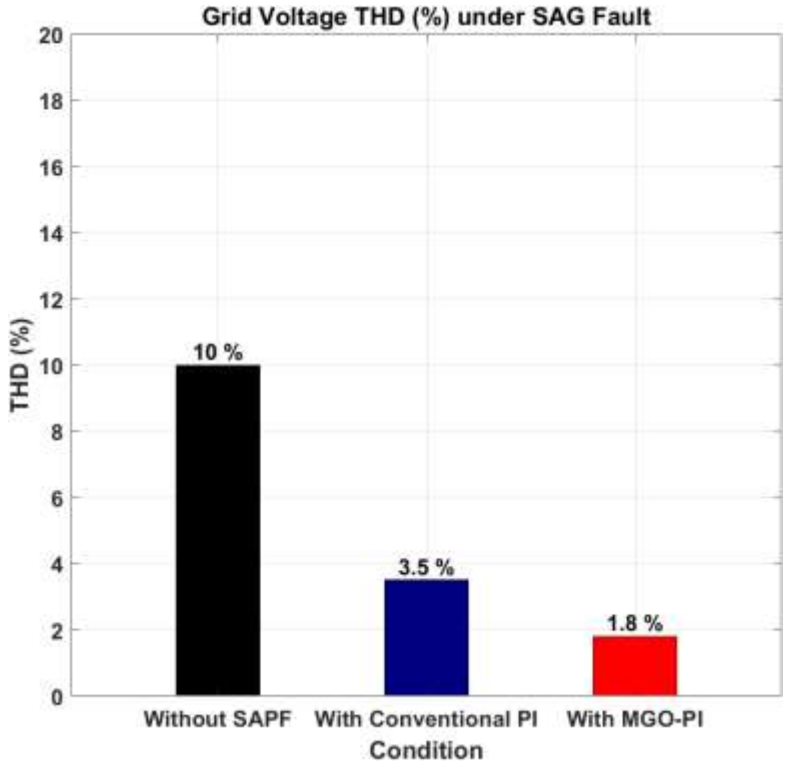

Fig.26(a). Grid Voltage THD (%) under SAG Fault

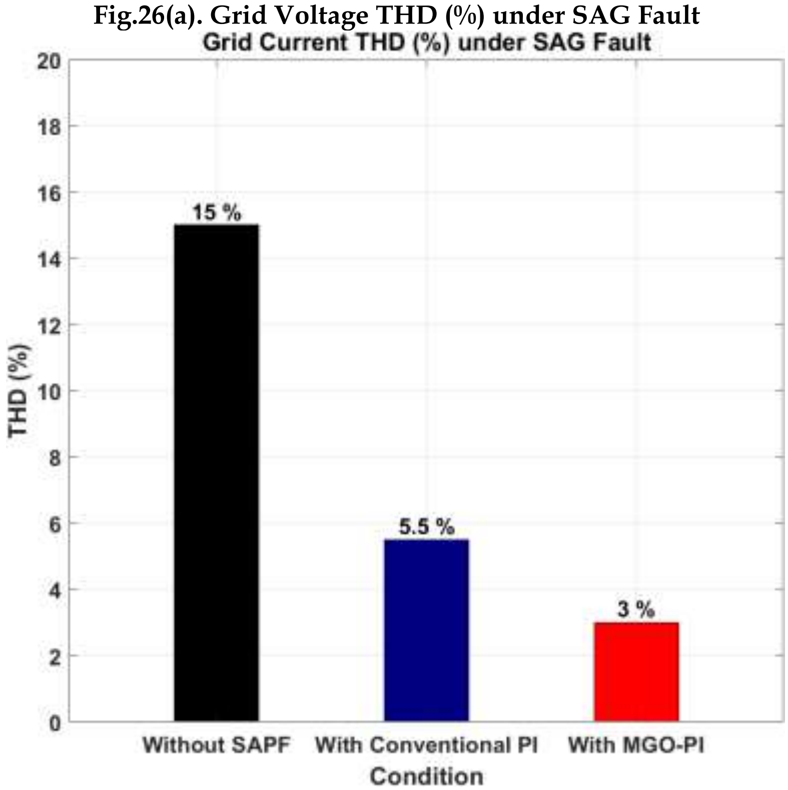

Fig.26(b). Grid Current THD (%) under SAG Fault

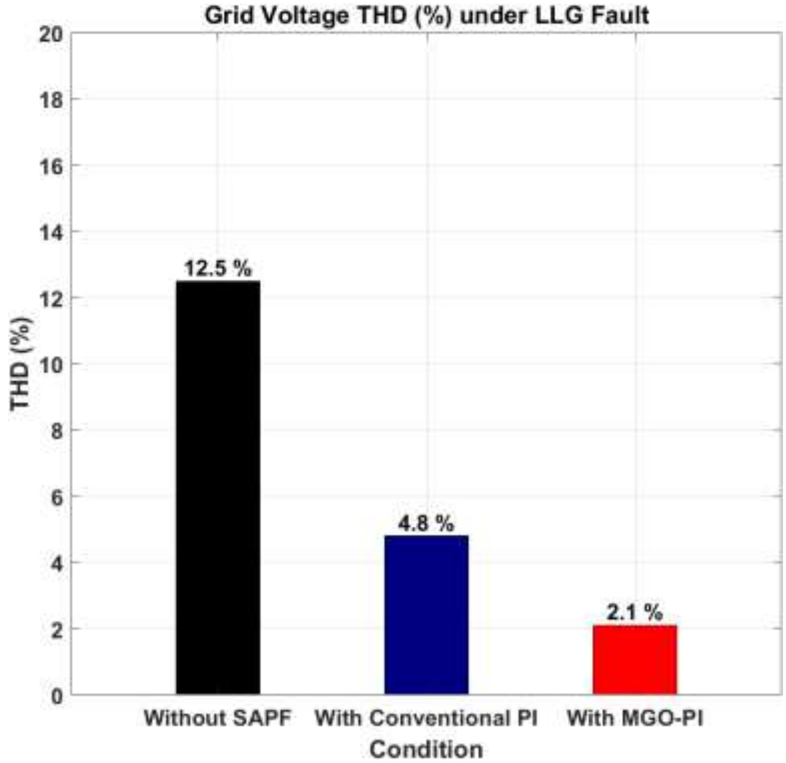

Fig.26(c). Grid Voltage THD (%) under LLG Fault

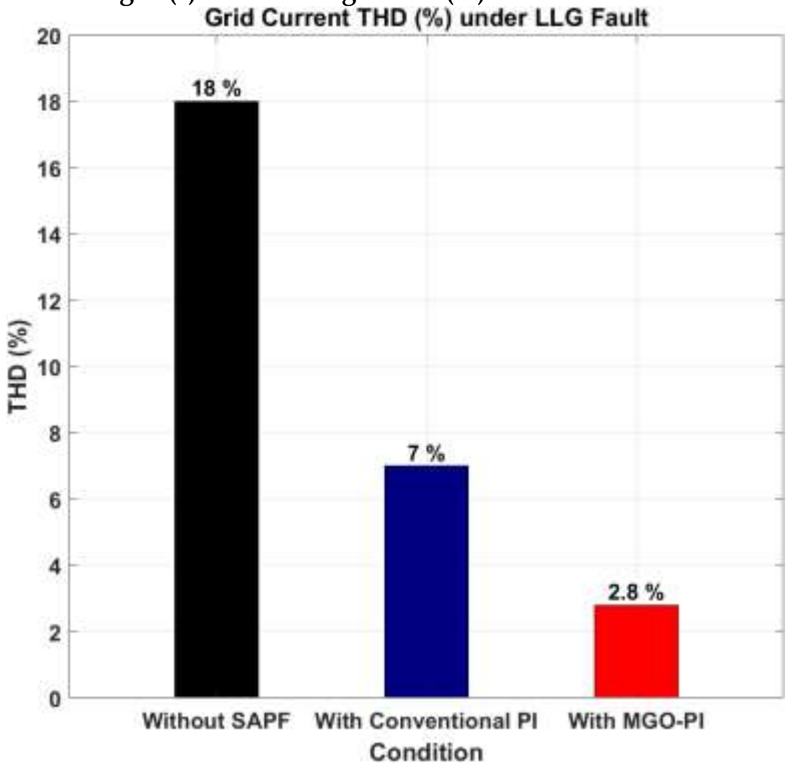

Fig.26(d). Grid Current THD (%) under LLG Fault

Table II. Comparative Numerical THD Values

Fault Type	**Signal Type**	**Without SAPF**	**With Conventional PI**	**With MGO-PI**
SAG	Grid Voltage	10 %	3.5 %	1.8 %
SAG	Grid Current	15 %	5.5 %	3 %

LLG	Grid Voltage	12.5 %	4.8 %	2.1 %
LLG	Grid Current	18 %	7 %	2.8 %

5 Research Findings

To optimally and dynamically adjust the Proportional Integral (PI) control parameters of the SAPF that drives the gate pulses of the inverter circuit, the Mountain Gazelle Optimiser (MGO) technique is utilised. The suggested technique has been applied in grid-tied MG configurations consisting of photovoltaic and fuel cell-based RESs, battery-based energy storage systems and SAPF-based FACTS devices to improve power quality during significant disturbances like voltage SAG and LLG faults. The effectiveness of the proposed controller has been evaluated by comparing its results with the conventional PI control method. Various responses, including voltage at DC-link, voltage at terminal, deviation in voltage, frequency, power factor, THD, active power of the grid, reactive power of the grid, apparent power of the grid, grid's voltage without SAPF, grid phase voltage with SAPF, grid's current without SAPF and grid's phase current with SAPF, were obtained from the simulation. A meticulous evaluation of the results is carried out for the suggested MGO-tuned PI method, and a comprehensive conclusion of the research findings is summarised below. Compared to conventional PI, the suggested MGO-PI approach effectively minimises the ripples related to the output voltage and current responses for distributed renewable energy sources like PV and FC at the source side.

While the MGO algorithm demonstrates high optimisation capability, its application in this study is limited to offline PI controller tuning. The optimised gains are embedded into the SAPF controller before operation, ensuring zero computational burden in real-time microgrid deployment. This preserves the simplicity and practical feasibility of the PI control structure. Strategies such as reduced-order MGO, hybrid adaptive controllers, or gain-scheduled lookup tables can be explored for future real-time deployment. Hardware-in-the-Loop (HIL) simulation can also be pursued to assess the viability of real-time implementation.

The overall research findings are listed below systematically.

i. There is significantly less variation in the battery-based energy storage devices' output voltage and current when using the recommended MGO-PI controller compared to the PI conventional technique.
ii. An improved state of charge (SoC) is obtained by the proposed MGO-tuned PI method, which efficiently minimises age-related capacity loss while maintaining battery functionality and allowing for partial discharge.
iii. For the suggested controller technique, on the onset of SAG and LLG faults, the voltage at the DC-link, voltage at the terminal, deviation in voltage, power factor and frequency are approximately preserved constant.
iv. The proposed method effectively maintains the apparent power, reactive power, and active power nearly constant with less oscillation and fluctuation throughout the fault situations, improving the MG system's capacity to deliver power.
v. Enhanced control in maintaining MG's voltage and current stability by incorporating SAPF and further superior management of grid's voltage and current with SAPF's PI controller tuned by the proposed MGO controller.
vi. Effectiveness of the suggested MGO-tuned PI controller in harmonics mitigation and voltage fluctuation, which lowers the MG's total THD (according to IEEE norms) compared to conventional PI controllers.
vii. The proposed controller improves overall system efficiency and transient stability, reduces harmonics, and provides robust control over grid voltage and current.

6 Conclusion

Ensuring high power quality (PQ) in grid-connected microgrid (MG) systems remains a critical challenge due to the integration of diverse Renewable Energy Sources (RESs), nonlinear loads, and power electronic interfaces that introduce harmonics, voltage imbalance, and switching transients. This study addresses these challenges by proposing an intelligent optimization-based Shunt Active Power Filter (SAPF) control framework employing the Mountain Gazelle Optimizer (MGO) for optimal tuning of Proportional–Integral (PI) controller gains. The proposed MGO-tuned PI controller dynamically regulates inverter switching pulses to achieve superior compensation of reactive power, harmonic mitigation, and voltage stabilization within a hybrid PV–Fuel Cell–Battery-based MG configuration.

The MGO algorithm, inspired by the social dynamics of mountain gazelles, demonstrates strong global search capability through an effective balance between exploration and exploitation phases. Its derivative-free nature, adaptive search mechanism, and high convergence efficiency make it well suited for nonlinear, high-dimensional optimization problems in power systems. Simulation studies conducted in the MATLAB/Simulink environment confirm that the proposed MGO-PI controller substantially outperforms the conventional PI method under severe PQ disturbances, including voltage SAG and Line-to-Line-to-Ground (LLG) faults. The controller ensures stable DC-link voltage, improved power factor, and reduced Total Harmonic Distortion (THD), thereby enhancing voltage stability, reliability, and overall system efficiency.

The results affirm that the intelligent MGO-based optimization framework significantly strengthens PQ indices at both the source and grid terminals, achieving IEEE 519-compliant harmonic levels. The proposed approach effectively mitigates current and voltage ripples, ensuring robust and reliable MG operation. Furthermore, its adaptability and computational simplicity highlight strong potential for real-time deployment and future integration with AI-driven adaptive control and machine learning-assisted optimization strategies for next-generation smart microgrid systems.

7 Future Directions

Building upon the promising outcomes of the proposed MGO-PI–based SAPF control strategy, several avenues for future research can be explored to further enhance system intelligence, adaptability, and real-time performance in microgrid environments:

i. Comparative Benchmarking: Conduct an extensive comparative analysis of the proposed MGO-PI controller with other state-of-the-art optimization algorithms, Artificial Neural Network (ANN)-based SAPF controllers, and hybrid intelligent control strategies to benchmark metaheuristic and learning-based methods.

ii. AI- and ML-Driven Control Frameworks: Develop more advanced and self-adaptive control architectures that integrate Artificial Intelligence (AI) and Machine Learning (ML) for real-time prediction, decision-making, and dynamic PQ optimization in complex microgrids.

iii. Demand Response and Predictive Optimization: Incorporate intelligent demand response and predictive scheduling algorithms to enhance energy management, load balancing, and operational optimization of distributed generation systems.

iv. Hybrid Energy Storage Integration: Investigate the integration of hybrid energy storage technologies (e.g., Li-ion batteries, supercapacitors, flywheels) to improve energy efficiency, transient stability, and power continuity during dynamic grid conditions.

v. Multi-Source Renewable Expansion: Extend the hybrid renewable architecture by incorporating additional Distributed Generation (DG) sources such as wind, biomass, and microturbines alongside PV and FC units to increase system flexibility and resilience.

vi. Advanced PQ Disturbance Mitigation: Explore the detection, analysis, and mitigation of other severe PQ anomalies—such as voltage swell, notching, flicker, and transient disturbances—using adaptive and intelligent control algorithms.

Appendix

Table III. System Parameters

PV array	**Fuel Cell (PEMFC)**	**Battery (Li-Ion type)**	**SAPF**
Max. power: 213.15 watt, Parallel strings: 40, Cells per module: 10, OC voltage: 36.3 volt, SC current: 7.84 amp, Light generated current: 7.86 A, Shunt Resistance: 313.05 ohm, Series resistance: 0.3938 ohm	Nominal stack power: 50000 watts, Resistance of fuel cell: 0.66404 ohm, Nernst voltage of cell: 1.1342 volts, System temperature: 338 Kelvin, Air supply pressure: 1 bar	Nominal voltage: 400 volts, Rated capacity: 20000 Ah, Initial state of charge: 40%, Battery response time: 0.03 sec	DC side capacitance: 43 µF, Filter coupling Inductance: 1.34 mH, Proportional gain K_p: 0.1, Integral gain K_i: 0.0015, V_{DC_ref} : 450 volt

References

[1] S. Choudhury and P. K. Rout, "Adaptive fuzzy logic based MPPT control for PV system under partial shading condition," Int. J. Renew. Energy Res., vol. 5, pp. 1252–1263, 2015.

[2] A. S. Nayak, D. P. Acharya, and S. Choudhury, "Photovoltaic Cell with Shunt Active Power Filter for Harmonic Cancelation Using Modified PSO-Based PI Controller," in Advances in Electrical Control and Signal Systems, Singapore: Springer, 2020, pp. 455–467.

[3] G. K. Sahoo et al., "Scaled conjugate-artificial neural network-based novel framework for enhancing the power quality of grid-tied microgrid systems," Alexandria Eng. J., vol. 80, pp. 520–541, 2023.

[4] X. Lü, Y. Qu, Y. Wang, C. Qin, and G. Liu, "A comprehensive review on hybrid power system for PEMFC-HEV: Issues and strategies," Energy Convers. Manag., vol. 171, pp. 1273–1291, 2018.

[5] D. P. Acharya et al., "Power quality improvement in a fuel-cell based micro-grid with shunt active power filter," Int. J. Renew. Energy Res., vol. 10, no. 3, pp. 1071–1082, 2020.

[6] S. Choudhury, "Review of energy storage system technologies integration to microgrid: Types, control strategies, issues, and future prospects," J. Energy Storage, vol. 48, Art. no. 103966, 2022.

[7] S. Nyamathulla and C. Dhanamjayulu, "A review of battery energy storage systems and advanced battery management system for different applications: Challenges and recommendations," J. Energy Storage, vol. 86, Art. no. 111179, 2024.

[8] C. Subhashree and N. Khandelwal, "A Novel Weighted Superposition Attraction Algorithm-based Optimization Approach for State of Charge and Power Management of an Islanded System with Battery and SuperCapacitor-based Hybrid Energy Storage System," IETE J. Res., vol. 69, pp. 825–830, 2020.

[9] Y. Hoon et al., "Shunt active power filter: A review on phase synchronization control techniques," Electronics, vol. 8, no. 7, Art. no. 791, 2019.

[10] E. H. George and E.-C. Gkampoura, "Reviewing usage, potentials, and limitations of renewable energy sources," Energies, vol. 13, Art. no. 2906, 2020.

[11] J. S. Ali et al., "Power System Stability with High Penetration of Renewable Energy Sources: Challenges, Assessment, and Mitigation Strategies," IEEE Access, 2025.

[12] M. Yessef et al., "Experimental validation of feedback PI controllers for multi-rotor wind energy conversion systems," IEEE Access, 2024.

[13] M. Sanaei et al., "Unbalance mitigation strategy and power quality improvement in microgrids using a state feedback controller and voltage profile improvement with an electric spring," Front. Energy Res., vol. 13, Art. no. 1545147, 2025.

[14] S. Tyagi, B. Singh, and S. Das, "Control of interlinking converter for power quality improvement in hybrid microgrid," IEEE Trans. Ind. Electron., 2024.

[15] K. Kanchana et al., "Advancing microgrid power quality: integration of GRU-based control in PV-UPQC systems," Electr. Eng., vol. 107, no. 1, pp. 223–248, 2025.

[16] J. P. Srividhya et al., "Power quality enhancement in smart microgrid system using convolutional neural network integrated with interline power flow controller," Electr. Eng., vol. 106, no. 6, pp. 6773–6796, 2024.

[17] C. Shravani and R. L. Narasimham, "Synergetic UPQC application for power quality enhancement in microgrid distribution system: SCSO approach," e-Prime Adv. Electr. Eng. Electron. Energy, vol. 10, Art. no. 100794, 2024.

[18] G. V. B. Kumar, K. Palanisamy, and E. De Tuglie, "Ramp-rate control for power quality improvement of renewable grid-integrated microgrid with hybrid energy storage system," Front. Energy Res., vol. 12, Art. no. 1387908, 2024.

[19] M. Abasi et al., "Power flow and power quality improvement of a residential-industrial microgrid using 72-pulse inverter-based UIPC," Int. J. Electr. Power Energy Syst., vol. 164, Art. no. 110449, 2025.

[20] M. Y. Artemenko et al., "Power Quality Assessment and Improvement of Grid-tied Distributed Generation Systems," in Electric Vehicles and Distributed Generation-Microgrid, River Publishers, 2025, pp. 89–146.

[21] J. He, Y. W. Li, and F. Blaabjerg, "Flexible microgrid power quality enhancement using adaptive hybrid voltage and current controller," IEEE Trans. Ind. Electron., vol. 61, no. 6, pp. 2784–2794, 2013.

[22] B. Cao et al., "Hybrid microgrid many-objective sizing optimization with fuzzy

decision," IEEE Trans. Fuzzy Syst., vol. 28, no. 11, pp. 2702–2710, 2020.

[23] M. L. T. Zulu, R. Sarma, and R. Tiako, "Modified Fuzzy Logic and Artificial Bee Colony: An Artificial Intelligence Approach to Optimization and Power Quality Improvement in an MPPT-Based System," Scientific African, 2025, Art. no. e02690.

[24] A. R. Jarwar et al., "High dynamic performance power quality conditioner for AC microgrids," IET Power Electron., vol. 12, no. 3, pp. 550–556, 2019.

[25] E. Hernández-Mayoral et al., "A comprehensive review on power-quality issues, optimization techniques, and control strategies of microgrid based on renewable energy sources," Sustainability, vol. 15, no. 12, Art. no. 9847, 2023.

[26] P. Ray, S. R. Das, S. Choudhury, and D. P. Acharya, "Performance Improvement of Microgrid with Strategic Control of Distributed Energy Resources Integrated UPQC," IEEE Transactions on Industry Applications, 2025.

[27] A. N. B. Alsammak, Z. M. T. Salleh, and H. A. Mohammed, "A review on enhancing power system transient stability using static VAR compensator-based intelligent control," Journal of Robotics and Control (JRC), vol. 6, no. 1, pp. 396–405, 2025.

[28] S. Kumar, A. Gupta, and R. K. Bindal, "Power quality investigation of a grid tied hybrid energy system using a D-STATCOM control and grasshopper optimization technique," Results in Control and Optimization, vol. 14, Art. no. 100368, 2024.

[29] S. Choudhury, "Flywheel energy storage systems: A critical review on technologies, applications, and future prospects," International Transactions on Electrical Energy Systems, vol. 31, no. 9, Art. no. e13024, 2021.

[30] M. Faraji, M. Y. El Amary, A. Eltamaly, and H. A. Gabbar, "Coordinated control of flywheel and battery energy storage systems for frequency regulation in diesel generator-based microgrid," IEEE Access, 2025.

[31] D.-E. A. Mansour, M. Abdel-Salam, M. A. Izzularab, A. A. Hanafy, and M. M. Radwan, "Development of a novel multifunctional superconducting device for performance enhancement of DC microgrids," Journal of Energy Storage, vol. 106, Art. no. 114723, 2025.

[32] S. Choudhury and G. K. Sahoo, "A critical analysis of different power quality improvement techniques in microgrid," e-Prime – Advances in Electrical Engineering, Electronics and Energy, 2024, Art. no. 100520.

[33] S. R. Das, D. P. Acharya, P. K. Rout, and S. Choudhury, "A comprehensive survey on different control strategies and applications of active power filters for power quality improvement," Energies, vol. 14, no. 15, Art. no. 4589, 2021.

[34] S. S. Patnaik and A. K. Panda, "Power quality enhancement using a novel SAPF control scheme employing high selectivity filter," International Journal of Emerging Electric Power Systems, vol. 25, no. 3, pp. 367–381, 2024.

[35] A. Bielecka, "Advanced control algorithm for shunt active power filter: Enhancing power quality in autonomous grids," Energies, vol. 17, no. 23, Art. no. 6186, 2024.

[36] A. Srivastava and S. Saravanan, "Harmonic mitigation using optimal active power filter for the improvement of power quality for an electric vehicle charging station," e-Prime – Advances in Electrical Engineering, Electronics and Energy, vol. 8, Art. no. 100527, 2024.

[37] E. Lahoussine, "Active disturbance rejection control of an islanded PV/wind/battery microgrid with power quality enhancement by SAPF," International Journal of Power Electronics and Drive Systems (IJPEDS), vol. 14, no. 3, pp. 1660–1674, 2023.

[38] S. Choudhury, A. K. Sahu, G. K. Sahoo, and S. R. Das, "Robust sliding mode controller and shunt active power filter for improvement of power quality indices of an autonomous microgrid," in Machine Vision and Augmented Intelligence: Select Proceedings of MAI 2022, Singapore: Springer Nature, 2023, pp. 345–356.

[39] B. Deffaf, A. Kherchouche, A. Mellit, T. A. Khezzar, and S. E. Zouzou, "Synergetic control for three-level voltage source inverter-based shunt active power filter to improve power quality," Energy Reports, vol. 10, pp. 1013–1027, 2023.

[40] M. U. M. Rao, P. S. Babu, K. R. Kiran, and R. S. Babu, "Stability improvement in microgrids using hybridization of RSFCL along with fuzzy based SAPF," International Journal on Interactive Design and Manufacturing (IJIDeM), 2022, pp. 1–8.

[41] S. Choudhury, D. P. Acharya, S. R. Das, and P. K. Rout, "Energy management and power quality improvement of microgrid system through modified water wave optimization," Energy Reports, vol. 9, pp. 6020–6041, 2023.

[42] P. Rajesh, K. R. Rajeswari, S. Durga, and S. Arulselvi, "An optimal hybrid control scheme to achieve power quality enhancement in microgrid connected system," International Journal of Numerical Modelling: Electronic Networks, Devices and Fields, vol. 35, no. 6, Art. no. e3019, 2022.

[43] H. F. Sindi, A. A. Mohammed, R. A. Saeed, and A. M. Al-Shaibani, "Robust control of adaptive power quality compensator in Multi-Microgrids for power quality enhancement using puzzle optimization algorithm," Ain Shams Engineering Journal, vol. 14, no. 8, Art. no. 102047, 2023.

[44] A. Aldosary, "Power quality conditioners-based fractional-order PID controllers using hybrid jellyfish search and particle swarm algorithm for power quality enhancement," Fractal and Fractional, vol. 8, no. 3, Art. no. 140, 2024.

[45] A. Kumar and J. Choudhary, "Power quality improvement of hybrid renewable energy systems-based microgrid for STATCOM: Hybrid-deep-learning model and Mexican axolotl dingo optimizer (MADO)," Engineering Research Express, vol. 5, no. 4, Art. no. 045031, 2023.

[46] S. C. Sahoo, A. K. Barik, and D. C. Das, "A novel Green Leaf-hopper Flame optimization algorithm for competent frequency regulation in hybrid microgrids," International Journal of Numerical Modelling: Electronic Networks, Devices and Fields, vol. 35, no. 3, Art. no. e2982, 2022.

[47] D. Zhang, M. Marzband, M. M. Alyami, S. Khormali, and M. Asif, "An optimal methodology for optimal controlling of a PEMFC connected to the grid based on amended penguin optimization algorithm," Sustainable Energy Technologies and Assessments, vol. 53, Art. no. 102401, 2022.

[48] M. Bhuyan, D. C. Das, and A. K. Barik, "Chaotic butterfly optimization algorithm based cascaded PI-TID controller for frequency control in three-area hybrid microgrid system," Optimal Control Applications and Methods, vol. 44, no. 5, pp. 2595–2619, 2023.

[49] S. K. Dash and P. K. Ray, "Power quality improvement utilizing PV fed unified power quality conditioner based on UV-PI and PR-R controller," CPSS Transactions on Power Electronics and Applications, vol. 3, no. 3, pp. 243–253, 2018.

[50] G. Sinha, P. K. Goswami, and S. K. Sharma, "A comparative strategy using PI and fuzzy controller for optimization of power quality control," Indonesian Journal of Electrical Engineering and Informatics (IJEEI), vol. 6, no. 1, pp. 118–124, 2018.